



Depth-extrapolation of field-scale soil moisture time series derived with cosmic-ray neutron sensing using the SMAR model

Daniel Rasche¹, Theresa Blume¹, and Andreas Güntner^{1,2}

¹GFZ German Research Centre for Geosciences, Section Hydrology, 14473, Potsdam, Germany

²University of Potsdam, Institute of Environmental Sciences and Geography, 14476, Potsdam, Germany

Correspondence: Daniel Rasche (daniel.rasche@gfz-potsdam.de)

Abstract. Soil moisture measurements at the field-scale are highly beneficial for different hydrological applications including the validation of space-borne soil moisture products, landscape water budgeting or multi-criteria calibration of rainfall-runoff models from field to catchment scale. Many of these applications require information on soil water dynamics in deeper soil layers. Cosmic-ray neutron sensing (CRNS) allows for non-invasive monitoring of field-scale soil moisture across several hectares around the instrument but only for the first few tens of centimeters of the soil. Simple depth-extrapolation approaches often used in remote sensing applications may be used to estimate soil moisture in deeper layers based on the near-surface soil moisture information. However, most approaches require a site-specific calibration using depth-profiles of in-situ soil moisture data, which are often not available. The physically-based soil moisture analytical relationship SMAR is usually also calibrated to sensor data, but could be applied without calibration if all its parameters were known. However, in particular its water loss parameter is difficult to estimate. In this paper, we introduce and test a simple modification of the SMAR model to estimate the water loss in the second layer based on soil physical parameters and the surface soil moisture time series. We apply the model at a forest site with sandy soils with and without calibration. Comparing the model results against in-situ reference measurements down to depths of 450 cm shows that the SMAR models both with and without modification do not capture the observed soil moisture dynamics well. The performance of the SMAR models nevertheless meets a previously used benchmark RMSE of $\leq 0.06 \text{ cm}^3 \text{ cm}^{-3}$ in both, calibrated and uncalibrated scenarios. Only with effective parameters in a non-physical range, a better model performance could be achieved. Different transfer functions to derive surface soil moisture from CRNS do not translate into markedly different results of the depth-extrapolated soil moisture time series simulated with SMAR. However, a more accurate estimation of the sensitive measurement depth of the CRNS improved the soil moisture estimates in the second layer. Despite the fact that the soil moisture dynamics are not well represented at our study site using physically reasonable parameters, the modified SMAR model may provide valuable first estimates of soil moisture in a deeper soil layer derived from surface measurements based on stationary and roving CRNS as well as remote sensing products where in-situ data for calibration are not available.



1 Introduction

Soil moisture is a key parameter in the hydrological cycle (e.g., Vereecken et al., 2008, 2014; Seneviratne et al., 2010). It controls several aspects of the environment such as soil infiltration, runoff dynamics, plant growth and biomass production which in turn influence evapotranspiration as well as the climatic conditions on varying spatio-temporal scales (see reviews by e.g., Daly and Porporato, 2005; Vereecken et al., 2008; Seneviratne et al., 2010; Wang et al., 2018). Thus, information on soil water dynamics at the field-scale have great importance for various larger-scale hydrological applications ranging from landscape water budgeting to multi-criteria calibration approaches in rainfall-runoff modeling. However, due to the high spatio-temporal variability of soil water content (Famiglietti et al., 2008; Vereecken et al., 2014) which is highest in surface soil layers (Babaeian et al., 2019), measuring field-scale soil moisture and its dynamics proves difficult based on invasive point-scale soil moisture measurement methods as for example reviewed in Vereecken et al. (2014) and Babaeian et al. (2019). For instance, the installation of electromagnetic point sensors measuring at high temporal resolution would require a very large number of sensors to obtain a representative field-scale average (Babaeian et al., 2019). Additionally, sensor networks are not always feasible as agricultural management practices hamper a permanent installation of point sensors (Stevanato et al., 2019). As a consequence, extensive point sensor networks which allow for the estimation of field-scale soil moisture are often restricted to a rather small number of research related monitoring sites such as the Terrestrial Environmental Observatories (TERENO, www.tereno.net) in Germany (e.g., Zacharias et al., 2011; Bogena et al., 2018; Kiese et al., 2018; Heinrich et al., 2018).

Kodama et al. (1979), Kodama et al. (1985) and Dorman (2004) suggested the potential of naturally occurring secondary neutrons produced by high-energy cosmic rays for estimating soil and snow water. About a decade ago Zreda et al. (2008); Desilets et al. (2010), introduced a methodological framework for soil moisture estimation using cosmic-ray neutrons. The cosmic-ray neutron sensing (CRNS) approach is a non-invasive geophysical method for estimating representative field-scale soil moisture (Schrön et al., 2018b) based on the measurement of cosmic-ray neutrons which are inversely related to the amount of hydrogen in the vicinity of the neutron detector. As soil water is the largest pool of hydrogen in the footprint of the neutron detector in most terrestrial environments, CRNS allows for the measurement of integrated soil moisture of several hectares around the instrument and the first decimetres of the soil (e.g., Zreda et al., 2008; Desilets et al., 2010; Köhli et al., 2015; Schrön et al., 2017).

Estimating soil moisture using CRNS has a high potential for various hydrological applications, which require soil moisture observations at the field-scale. Several studies demonstrate the potential of CRNS-derived soil moisture estimates for example for a comparison with satellite derived soil moisture products, their validation and the improved calibration of environmental models (e.g., Holgate et al., 2016; Montzka et al., 2017; Iwema et al., 2017; Duygu and Akyürek, 2019; Dimitrova-Petrova et al., 2020). Besides stationary CRNS probes for the retrieval of field scale soil moisture time series, roving CRNS-devices have been successfully used, mapping CRNS-derived surface soil moisture in even larger areas with instruments mounted on vehicles (e.g., McJannet et al., 2017; Schrön et al., 2018a; Vather et al., 2019) and (Fersch et al., 2018) illustrate potential synergies between CRNS, airborne radar and in-situ point sensor networks for soil moisture estimation across spatial scales. Due to the sensitivity of CRNS to any hydrogen in the measurement footprint, snow monitoring (e.g., Schattan et al., 2017, 2019; Gugerli



et al., 2019), irrigation management (e.g., Li et al., 2019a) as well as biomass estimation (e.g., Baroni and Oswald, 2015; Tian et al., 2016; Jakobi et al., 2018; Vather et al., 2020) pose further fields of application and are reviewed in Andreasen et al. (2017).

60 Although the large areal footprint of the CRNS-instrument allows estimating field-scale integral soil moisture, the CRNS-derived time series lack soil moisture information from greater depths. However, soil moisture at these greater depths becomes highly relevant as soon as the rooting depth of crops or forest extends past the first decimeters. The maximum rooting depth and hence, root zone extent as well as root density along the soil profile varies with vegetation type and biome (e.g., Canadell et al., 1996; Jackson et al., 1996). According to Jackson et al. (1996), on global average across all biomes, the 75 percent of
65 plant roots occur in the first 40 centimetres of the soil, which would be largely covered by the CRNS. However, the global average maximum rooting depth, and thus, root zone depth is about 4.6 m (Canadell et al., 1996) where the rooting depth also depends on prevailing soil hydrological conditions (Fan et al., 2017). Even grassy vegetation and crops can have rooting depths of more than 200 cm (Canadell et al., 1996), thus exceeding the measurement depth of CRNS. Deep roots play a significant role for the water supply of plant ecosystems especially during dry conditions (Canadell et al., 1996) i.e. through hydraulic
70 redistribution (see e.g., Neumann and Cardon, 2012) or increased root water uptake from deeper soil layers under drought conditions (Maysonnave et al., 2022). Furthermore, plant species influence infiltration and vertical soil moisture patterns through species dependent root distributions (e.g. Jost et al., 2012) and horizontal soil moisture patterns through species dependent evapotranspiration and interception rates (e.g. Schume et al., 2003). Hence, field-scale soil water information from the deeper vadose zone overcoming these smaller scale heterogeneities can be important for the quantification of water storage variations,
75 potential influences on vegetation dynamics, matter fluxes and the characterization of the local hydrological cycle.

Given the importance of soil moisture in the deeper root zone, extending CRNS-measurements to greater depths is of high importance for broadening the applicability of CRNS for soil water estimations (Peterson et al., 2016). Numerous studies extrapolate surface soil moisture time series to greater depths using different empirical approaches (e.g., Zhang et al., 2017; Li and Zhang, 2021) including regression analyses, machine learning techniques or other approaches such as the soil water
80 index (SWI) (Wagner et al., 1999; Albergel et al., 2008). Few studies address the depth-extrapolation of field-scale CRNS-derived soil moisture time series (e.g., Peterson et al., 2016; Zhu et al., 2017; Nguyen et al., 2019; Franz et al., 2020) to the shallow root zone (approx. 100 cm) by applying and comparing extrapolation approaches with the SWI being the most commonly used approach (e.g., Peterson et al., 2016; Dimitrova-Petrova et al., 2020; Franz et al., 2020). All these approaches require reference soil moisture information in the depth of interest to either build an empirical model or calibrate the depth-
85 extrapolated soil moisture time series. This information may not always be available in sufficient quantity and quality. In contrast, the physically-based soil moisture analytical relationship (SMAR) (Manfreda et al., 2014), applied and modified in recent studies (e.g., Faridani et al., 2017; Baldwin et al., 2017, 2019; Gheybi et al., 2019; Zhuang et al., 2020; Farokhi et al., 2021), allows for the extrapolation of daily surface soil moisture information to a second, lower soil layer by solely relying on soil physical information and a water loss term. This method does not require calibration if the environmental parameters are
90 known.



Against this background, we investigate the potential to depth-extrapolate hourly and daily surface soil moisture time series without calibration and thus without the need for reference soil moisture information in the depth of interest by applying the SMAR algorithm at a highly equipped study site in the TERENO-NE observatory located the lowlands of north-eastern Germany. While soil physical parameters may be determined from soil analyses, the water loss parameter describing the water loss per unit time from the second soil layer is more difficult to estimate. Therefore, we propose a simple modification of the SMAR algorithm to estimate the water loss term from soil physical characteristics and from the surface soil moisture time series derived from CRNS. We first compare the standard SMAR that uses a constant, calibrated water loss term (calibrated against in-situ reference sensors) with the modified, uncalibrated SMAR that uses the estimated water term loss for different depths of the second soil layer down to 450 cm depth. Secondly, we calibrate all soil parameters in the original and modified version of the SMAR model in order to assess its best possible performance at the study site for the given in-situ reference data. In addition, we apply different neutron-to-soil moisture transfer functions available to derive the surface soil moisture time series. This is done to assess which transfer function performs best and if a better CRNS-derived surface soil moisture time series translates into better estimates of the depth-extrapolated soil moisture. Lastly, we test the influence of the choice of the depth of first soil layer, i.e. the sensitive measurement depth of CRNS, on the goodness-of-fit of the depth-extrapolated soil moisture estimates.

2 Material and methods

2.1 Study site

The study site is located in the TERENO-NE observatory (Heinrich et al., 2018) in the young Pleistocene landscape of north-eastern Germany (Fig. 1). The site hosts the CRNS sensor „Serrahn“ (Bogena et al., 2022). The site has a mean annual temperature of 8.8°C and mean annual precipitation of 591 mm per year, measured at the long-term weather station in Waren (in a distance of approximately 35 km) operated by the German Weather Service (station ID: 5349, period 1981–2010) (DWD - German Weather Service, 2020a, b). It is situated on the southern ascent of a glacial terminal moraine formed during the Pomeranian phase of the Weichselian glaciation in the Pleistocene (Börner, 2015). The dominating soil types in the vicinity of the sensor are Cambisols formed on aeolian sands with depths down to 450 cm deposited during the Holocene (Rasche et al., 2023). Continuing downwards, these are followed by deposited glacial till of the terminal moraine, glacio-fluvial sediments and glacial tills originating from earlier glaciations with the latter forming the aquitarde the upper groundwater aquifer with water level depths ranging between 13 and 14 m below the surface (Rasche et al., 2023). A mixed forest dominated by European beech (*Fagus sylvatica*) and Scots pine (*Pinus sylvestris*) is the dominant landcover type. A clearing covered by grassy vegetation can be found nearby.

In order to calibrate the CRNS sensor, soil samples were taken at different distances around the instrument in February 2019 as shown in Fig. 1. Soil samples were taken in 5 cm depth increments from 0–35 cm using a split tube sampler containing sampling rings in order to derive soil moisture, soil physical characteristics, average grain size distributions, soil organic matter and lattice water from laboratory analyses as shown in Tab. 1. Soil moisture and soil bulk density were determined from oven-

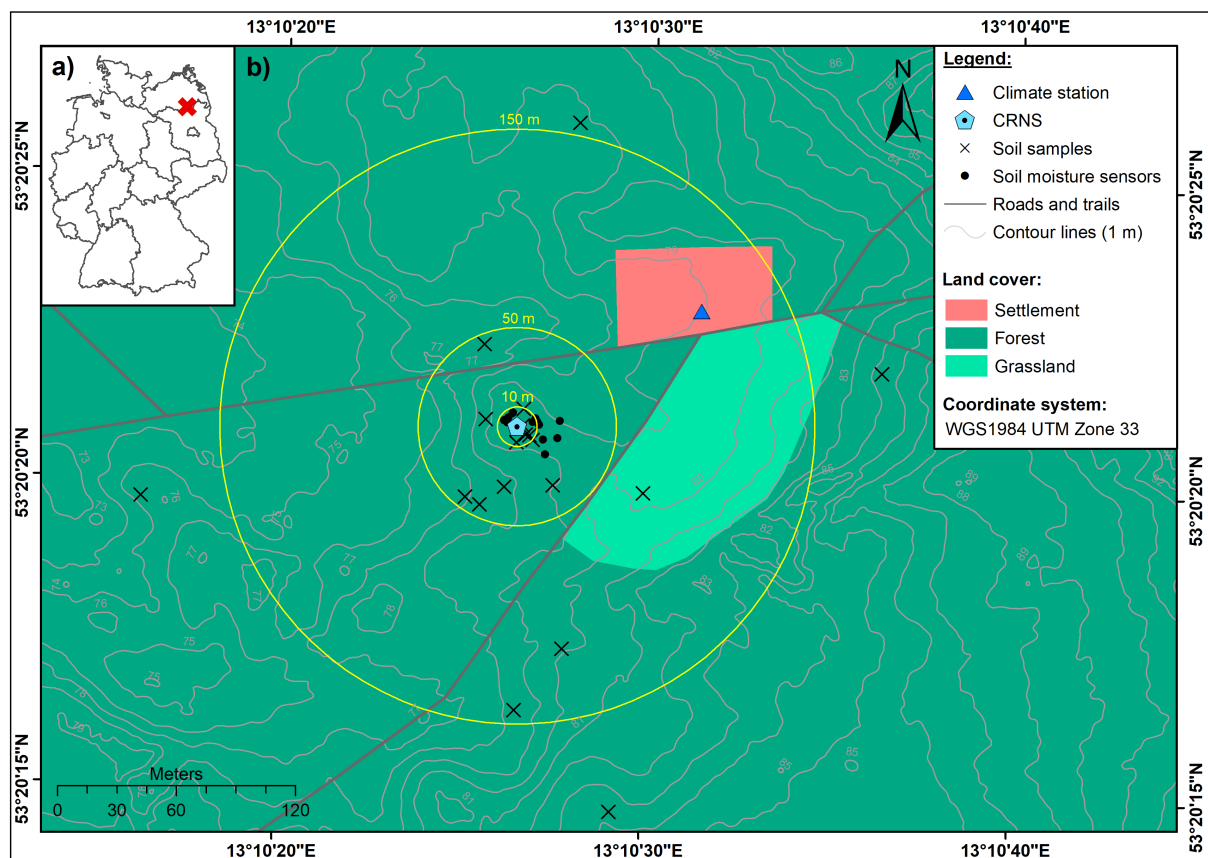


Figure 1. Location of the study area within Germany (a) and location of the CRNS observation site „Serrahn“ (b) (digital elevation model: LAIV-MV - State Agency for Interior Administration Mecklenburg-Western Pomerania (2011), land cover: BKG - German Federal Agency for Cartography and Geodesy (2018)).

drying at 105°C for 12 h and gravimetric analyses of all individual soil samples. Subsequent loss-on-ignition analyses at 550
125 and 1000°C with a duration of 24 h were used to determine the amount of soil organic matter and lattice water from bulk
samples per depth assuming that no inorganic carbon is present in the acidic aeolian sands. Soil porosity was estimated based
on the material density of quartz (2.65 g cm^{-3}) and corrected for the amount of soil organic matter based on the density of
cellulose (1.5 g cm^{-3}).

In addition to the stationary CRNS instrument, the study site is equipped with a groundwater observation well, a weather
130 station and a network of in-situ point-scale soil moisture sensor profiles (type SMT100; Truebner GmbH, Germany). A total
of 59 in-situ soil moisture sensors is deployed in depths down to 450 cm depth with 12 sensors in 10 cm, 6 sensors in 20 cm, 8
sensors in 30 cm, 8 sensors in 50 cm, 6 sensors in 70 cm, 4 sensors in 130 cm, 7 sensors in 200 cm, 4 sensors in 300 cm as well



as 450 cm. The sensors are located in distances up to 22 m from the CRNS instrument and continuously monitor the volumetric soil moisture content based on the manufacturer's calibration function.

Table 1. Soil physical characteristics at the CRNS site Serrahn obtained from laboratory analyses of soil samples (Rasche et al., 2023, modified). Below the maximum sampling depth of 35 cm and down to the maximum depth of the aeolian sand deposits, the soil physical are assumed to have the same soil physical parameters as the layer between 30 and 35 cm. The soil moisture content at field capacity and wilting point were taken from tabulated values in Sponagel et al. (2005) according to the respective soil grain size class (medium-fine sand) and the soil bulk density of the individual layers.

| Depth [cm] | Grain size fractions [weight-%] | | | | | Bulk density [g cm ⁻³] | Porosity [-] | Organic matter [g g ⁻¹] | Lattice water [g g ⁻¹] | Field capacity [cm ³ cm ⁻³] | Wilting point [cm ³ cm ⁻³] |
|---------------|------------------------------------|-------------|---------------|----------------|------------|---------------------------------------|-----------------|--|---------------------------------------|---|--|
| | > 2 mm | 2 - 0.63 mm | 0.63 - 0.2 mm | 0.2 - 0.063 mm | < 0.063 mm | | | | | | |
| 0–5 | 2.7 | 19.7 | 42.2 | 33.7 | 2.1 | 0.24 | 0.91 | 0.32 | 0.003 | 0.16 | 0.06 |
| 5–10 | 1.1 | 8.7 | 43.5 | 45.7 | 2.4 | 0.77 | 0.70 | 0.10 | 0.002 | 0.16 | 0.06 |
| 10–15 | 0.7 | 7.2 | 41.5 | 47.9 | 2.8 | 1.25 | 0.52 | 0.05 | 0.002 | 0.16 | 0.06 |
| 15–20 | 1.2 | 7.8 | 38.7 | 44.3 | 2.2 | 1.43 | 0.45 | 0.02 | 0.002 | 0.14 | 0.05 |
| 20–25 | 1.7 | 7.7 | 42.2 | 46.5 | 2.2 | 1.55 | 0.41 | 0.02 | 0.002 | 0.14 | 0.05 |
| 25–30 | 1.7 | 8.5 | 43.5 | 45.4 | 1.2 | 1.59 | 0.40 | 0.01 | 0.002 | 0.12 | 0.04 |
| 30–35 | 1.1 | 8.0 | 42.8 | 46.8 | 1.5 | 1.63 | 0.38 | 0.01 | 0.002 | 0.12 | 0.04 |
| 35–450 | 1.1 | 8.0 | 42.8 | 46.8 | 1.5 | 1.63 | 0.38 | 0.01 | 0.002 | 0.12 | 0.04 |

135 2.2 Field-scale surface soil moisture derived with CRNS

Secondary neutrons are produced by primary cosmic-rays interacting with matter in the atmosphere and in the ground. Depending on their energy level, secondary neutrons may be classified as fast (0.1-10 MeV), epithermal (> 0.25-100 keV) and thermal neutrons (< 0.25 eV) (e.g., Köhli et al., 2015; Weimar et al., 2020). Cosmic-ray neutron sensing for soil moisture estimation relies on the amount of neutrons in the epithermal energy range produced by nuclear evaporation in the atmosphere and ground
 140 (Köhli et al., 2015). Epithermal neutrons are sensitive to elastic scattering by collision with hydrogen and are further moderated to thermal neutrons (< 0.25 eV). Thus, the amount of epithermal neutrons detected by the instrument is inversely correlated with the amount of hydrogen in the sensitive measurement footprint of the sensor.

Epithermal neutron counts detected by the instrument are influenced by atmospheric pressure, the amount of primary high-energy cosmic-ray neutrons entering the earth's atmosphere from space (Zreda et al., 2012) as well as variations of absolute
 145 air humidity (Rosolem et al., 2013) and need to be corrected for these influencing factors before soil moisture information can be derived. In this study, we use the correction procedure for air pressure and incoming primary cosmic-ray flux presented in Zreda et al. (2012). The correction factor for the shielding effect of the atmosphere can be calculated from local air pressure measurements where the attenuation length L is set to 135.9 g cm⁻² for the study area (Heidbüchel et al., 2016). The correction factor for the incoming high-energy primary neutron flux was obtained from hourly pressure and efficiency corrected primary
 150 neutron intensities (cps) of the Jungfraujoch neutron monitor (JUNG, www.nmdb.eu). Furthermore, the neutron data was corrected for the influence of absolute air humidity introduced by Rosolem et al. (2013). The absolute humidity is calculated



from relative humidity and temperature observations of the weather station at the observation site according to Rosolem et al. (2013). For all correction approaches, the time series averages of air pressure, incoming radiation and air humidity are used as the required reference values. Finally, a 25 h moving average filter is applied to the corrected neutron time series to reduce noise and uncertainty in the data (e.g., Schrön et al., 2018b).

$$\theta_{\text{Standard}} = \left(\left(\frac{\tilde{a}_0 \left(1 - \frac{N_{\text{pih}}}{N_{\text{max}}} \right)}{\tilde{a}_1 - \frac{N_{\text{pih}}}{N_{\text{max}}}} \right) \times \frac{\rho_{\text{soil}}}{\rho_{\text{water}}} \right) - (\theta_{\text{SOM}} + \theta_{\text{LW}}), \quad (1)$$

where

$$\tilde{a}_0 = -a_2, \quad (2)$$

$$\tilde{a}_1 = \frac{a_1 a_2}{a_0 + a_1 a_2}, \quad (3)$$

$$N_{\text{max}} = N_0 \cdot \frac{a_0 + a_1 a_2}{a_2}. \quad (4)$$

Desilets et al. (2010) introduced a transfer function to convert neutron counts into soil moisture by calibration against reference measurements. Although other approaches exist (e.g., Franz et al., 2013; Köhli et al., 2021), the Desilets's equation became the methodological standard and can be rewritten as eq. (1) – (4) (Köhli et al., 2021) with $a_0 = 0.0808$, $a_1 = 0.372$, $a_2 = 0.115$ and N_0 being a local calibration parameter describing the neutron intensity above dry soil (Desilets et al., 2010). As observed epithermal neutron intensities are sensitive to any hydrogen present in the measurement footprint, the water equivalent of soil organic matter θ_{SOM} and the amount of lattice water θ_{LW} in $\text{cm}^3 \text{cm}^{-3}$ need to be subtracted. Additionally, ρ_{soil} describes the average soil bulk density in the measurement footprint (g cm^{-3}) and ρ_{water} the density of water assumed to be 1 g cm^{-3} . In this neutron-to-soil moisture transfer function the neutron intensity corrected for variations in air pressure, incoming primary neutron flux and absolute humidity N_{pih} is used. However, the more recent study by Köhli et al. (2021) suggests that the influence of absolute air humidity and soil moisture on the observed epithermal neutron signal are interdependent, i.e. the shape of the neutron-soil moisture relationship changes with absolute humidity. The universal transport solution (UTS), eq. (5) – eq. (6), (Köhli et al., 2021) accounts for the changing relationship between neutrons and soil moisture under different conditions of absolute humidity.

$$N_{\text{pi}} = N_D \cdot \left(\frac{p_1 + p_2 \theta_{\text{total}}}{p_1 + \theta_{\text{total}}} \cdot (p_3 + p_4 h + p_5 h^2) + e^{-p_6 \theta_{\text{total}}} (p_7 + p_8 h) \right), \quad (5)$$

where



$$\theta_{\text{total}} = (\theta_{\text{UTS}} + \theta_{\text{SOM}} + \theta_{\text{LW}}) \cdot \frac{1.43 \text{ g cm}^{-3}}{\rho_{\text{soil}}} \quad (6)$$

The UTS is designed to describe the neutron intensity response caused by changes in total soil water content and absolute air humidity and therefore, the predicted neutron intensity represents the intensity corrected for variations in atmospheric pressure and incoming primary neutron flux N_{pi} . Soil moisture can be derived from the UTS using numerical inversion or a look-up table approach which is used in this study. Analogously to the standard transfer function, the UTS needs to be calibrated locally. The calibration parameter N_D may be interpreted as the average neutron intensity of the local neutron detector under the boundary conditions defined in the neutron transport simulations which were used to subsequently derive the UTS. θ_{total} describes the total water content comprising the sum of all below-ground hydrogen pools, namely the soil moisture content θ_{UTS} , θ_{SM} and θ_{LW} which is then scaled by ratio of the soil bulk used in the neutron transport simulations to derive the UTS (1.43 g cm^{-3}) and the local soil bulk density at the study site ρ_{soil} (Köhli et al., 2021). Different sets of shape-giving parameters $p_1 - p_{10}$ are available for the UTS in Köhli et al. (2021) and originate from the different neutron transport models used and whether a simple energy window threshold (thl) was used (parameter sets: URANOS thl, MCNP thl) to evaluate the neutron transport simulations or a more complex detector response function was applied (parameter sets: URANOS drf, MCNP drf). The latter mimics the response of a real neutron detector and is therefore expected to provide more accurate results. In the scope of this study, we investigate which of the two transfer functions and which parameter set of the UTS performs best in estimating surface soil moisture.

The CRNS footprint diameter as well as the integration depth decrease with i.e. increasing soil water content. The radius ranges between 130 and 240 m and the integration depth ranges between 15 and 83 cm during wet and dry conditions, respectively (Köhli et al., 2015). In addition, further factors may influence the footprint dimensions such as open water or topography (e.g., Köhli et al., 2015; Schattan et al., 2019; Mares et al., 2020). Consequently, reference measurements need to be depth-distance weighted according to the sensitivity of the CRNS instrument in order to match field observations of reference measurements when calibrating the two different transfer functions and derive soil moisture information from observed neutron intensities. In this study, we adapt the weighting procedure proposed by Schrön et al. (2017) which takes the total water content, average bulk density, absolute air humidity and vegetation height (set to 20 m) into account. Reference soil moisture information from the soil sampling campaign in February 2019 was weighted accordingly and used for calibrating both transfer functions. In a second step, the CRNS-derived soil moisture time series are compared to an analogously weighted average of all available in-situ soil moisture sensors in 10, 20 and 30 cm depth. In order to assess the impact of weighting procedure, the calibration is repeated using the arithmetic soil moisture average from soil samples and comparing the CRNS-derived soil moisture time series to the arithmetic average soil moisture time series from in-situ sensors.



205 2.3 Depth-extrapolation of surface soil moisture time series from CRNS

2.3.1 Modification of the SMAR model

To estimate depth-extrapolated soil moisture time series for a second, deeper soil layer from CRNS-derived surface soil moisture time series, the SMAR model is used. Introduced by Manfreda et al. (2014), it allows for the physically-based estimation of soil moisture in an adjacent second, lower soil layer from soil moisture information in a first, upper soil layer. SMAR is based on the relative saturation in the first and second layer s_1 (-) and s_2 (-), respectively, the relative saturation at field capacity s_{c1} (-) and wilting point s_{w2} (-). In order to transform values from $\text{cm}^3 \text{cm}^{-3}$ to relative saturation, the respective variables are divided by the porosity of the individual layer n_1 ($\text{cm}^3 \text{cm}^{-3}$) and n_2 ($\text{cm}^3 \text{cm}^{-3}$). After applying the SMAR model, the resulting relative saturation time series of the second layer s_2 (-) is transformed back to volumetric soil moisture in $\text{cm}^3 \text{cm}^{-3}$ by multiplication with n_2 ($\text{cm}^3 \text{cm}^{-3}$) and resulting in the depth-extrapolated soil moisture time series $\theta_{\text{Layer 2}}$. Soil moisture in layer 2 at time t is calculated with

$$s_2(t_i) = s_{w2} + (s_2(t_{i-1}) - s_{w2}) \cdot e^{-a \cdot (t_i - t_{i-1})} + (1 - s_{w2}) \cdot b \cdot y(t_i) \cdot (t_i - t_{i-1}), \quad (7)$$

where a and b depend on the vertical extent of the first layer (Zr_1 in mm) which begins at the soil surface, and the vertical extent of the second layer (Zr_2 in mm). Zr_2 is the difference between the maximum depth of the second soil layer and Zr_1 . The water loss term V_2 (mm t^{-1}) comprises the bulk water losses from the second layer due to percolation and evapotranspiration per unit time:

$$a = \frac{V_2}{(1 - s_{w2}) \cdot n_2 \cdot Zr_2}, \quad (8)$$

$$b = \frac{n_1 \cdot Zr_1}{(1 - s_{w2}) \cdot n_2 \cdot Zr_2}, \quad (9)$$

The fraction of saturation of the first layer that instantaneously infiltrates into the second layer $y(t_i)$ (-) is described as (e.g., Manfreda et al., 2014; Patil and Ramsankaran, 2018):

$$y(t_i) = \begin{cases} (s_1(t_i) - s_{c1}), & s_1(t_i) \geq s_{c1} \\ 0, & s_1(t_i) < s_{c1}. \end{cases} \quad (10)$$

The SMAR model can be applied using known soil physical and environmental variables. However, although the soil physical parameters may be estimated through pedotransferfunctions, using tabulated values or global soil databases (e.g. SoilGrids 2.0 (Poggio et al., 2021)), the bulk water loss from the second layer V_2 is more difficult to estimate. This hampers the use of SMAR



230 without calibration against reference soil moisture information in the depth of interest, i.e., in the deeper soil layer. To overcome
 this issue we modified and extended the SMAR model in order to estimate the V_2 based on simple soil physical, environmental
 variables and the surface soil moisture time series. A modification of the SMAR model with an extended definition of the water
 loss term V_2 has been suggested by Faridani et al. (2017) leading to an improved performance compared to the original SMAR
 model. As any modification makes the SMAR model more complex and potentially less easy to apply, our aim was to keep the
 235 added complexity to the model low by only including 3 additional parameters. These are the relative saturation at field capacity
 in the second layer sc_2 (-) and the cumulative root fraction to the maximum depth of the first and second layer R_1 (-) and R_2
 (-), respectively. The water loss term is then defined as the sum of evapotranspiration ET_2 (mm t^{-1}) and percolation P_2 (mm
 t^{-1}) from the second layer.

$$V_2 = ET_2 + P_2, \quad (11)$$

240 We adapt the suggestion of Manfreda et al. (2014) to make use of existing (surface) soil moisture time series to gain infor-
 mation about water loss from the soil by evapotranspiration at a study site. Here, we estimate the amount of evapotranspiration
 from the deeper layer ET_2 based on the difference between the current and past value of relative saturation of the first layer,
 by scaling the value to the dimension (i.e. extent) of second layer and by considering the difference in cumulative root fraction
 between both layers, assuming that root water uptake for ET is larger in the layer with more roots eq. (13). The required root
 245 fraction R (-) for maximum depth d (cm) of the first and second layer are derived from the empirical equation (eq. 12) for
 forest biomes presented in Jackson et al. (1996):

$$R = 1 - 0.970^d \quad (12)$$

Using eq. 13, ET_2 can only be estimated from the change in relative saturation in the first layer when 1) the relative saturation
 of the first layer s_1 decreases, 2) no infiltration into the second layer occurs and 3) the relative saturation of the second layer
 250 exceeds the relative saturation at wilting point. This means that both, surface evaporation and transpiration losses are scaled
 from the first layer to the second layer. Although surface evaporation is hardly relevant for the second layer due to its missing
 connection with the surface, this is a reasonable yet simplified approach because surface evaporation is a comparatively small
 component of total evapotranspiration in forests, with transpiration dominating ET (e.g., Li et al., 2019b; Paul-Limoges et al.,
 2020).

$$255 \quad ET_2(t_i) = \begin{cases} (s_1(t_i - 1) - s_1(t_i)) \cdot n_1 \cdot Zr_1 \cdot \frac{Zr_2}{Zr_1} \cdot \frac{(R_2 - R_1)}{R_1}, & s_1(t_i - 1) \geq s_1(t_i); y(t_i) > 0; s_2(t_i - 1) \leq s_{w2} \\ 0, & otherwise. \end{cases} \quad (13)$$

The amount of percolation P_2 from the second layer is estimated in analogy to the infiltration into this layer as an instantane-
 ous water loss when the relative saturation exceeds field capacity sc_2 (eq. 14).



$$P_2(t_i) = \begin{cases} (s_2(t_i - 1) - s_{c2}), & s_2(t_i - 1) \geq s_{c2} \\ 0, & s_2(t_i - 1) < s_{c2}. \end{cases} \quad (14)$$

260 2.3.2 Application of the SMAR model

We applied the SMAR model in its original form by calibrating the V_2 water loss term as a constant value. The calibration and evaluation was performed against an average soil moisture time series in the deeper layer derived from in-situ soil moisture sensors. All available in-situ sensor soil moisture time series per depth were averaged to derive average soil moisture time series per sensor depth. Subsequently, we calculated an average soil moisture time series for the second, deeper soil layer by weighting the averages per depth according to their representative layer extent (called reference time series in the following). For example, having soil moisture sensors installed in 30, 50 and 70 cm depth, the average soil moisture content per time step of all sensors installed in 50 cm is representative for the layer between 40 and 60 cm. The soil physical parameters assigned to the individual layers can be found in Tab, 1. The calibration is performed by minimising the root-mean square error (RMSE) between the depth-extrapolated soil moisture time series and the entire reference soil moisture time series in the second soil layer.

The original SMAR with calibrated V_2 and the modified SMAR model with estimated V_2 are applied to estimate a soil moisture time series in a second soil layer with a maximum depth below terrain surface of 70, 130, 200, 300 and 450 cm. In contrast, the modified SMAR model based on eq. 11–14 is applied using the same soil physical parameters but it does not require calibration of the V_2 water loss term.

In order to test if a better surface soil moisture time series translates to better extrapolated soil moisture values in the second layer, we apply the SMAR model using the CRNS-derived surface soil moisture estimated from the standard transfer function (eq. (1)) as well as using the UTS (eq. (5) – (6)) with the parameter set resulting in the highest goodness-of-fit expressed by the lowest RMSE.

The vertical extent of the first soil layer is defined according to the representative measurement depth of the CRNS-derived soil moisture time series. In first step, the model is tested using a depth of the first layer of 35 cm as the sensitive measurement depth of CRNS is often estimated to range between 30 and 40 cm. However, more accurate approaches exist to determine the sensitive measurement depth. In this study, we also calculate median CRNS measurement depth of the entire CRNS-soil moisture time series based on Schrön et al. (2017) and use it as the depth of the first soil layer in the SMAR model. According to Schrön et al. (2017), the sensitive measurement depth D_{86} is estimated using the calibrated CRNS-derived soil moisture time series for distances from 1 to 300 m around the instrument. Subsequent averaging allows for estimating the average measurement depth in the CRNS footprint for each time step of the time series. The time series median measurement depth D_{86} is then calculated for the soil moisture time series derived with the standard transfer function and the UTS. For both CRNS-derived soil moisture time series, the estimated median sensitive measurement depth is 20 cm and much smaller than



the rough initial estimate of 35 cm. As a consequence, we decided to apply the original and modified SMAR model with a first layer depth of both 20 cm and 35 cm to investigate the effect on the resulting depth-extrapolated soil moisture time series.

In summary, for each maximum depth of the second soil layer, the SMAR model is applied in its original form based on calibration and in the modified version presented in this study which does not require calibration. This is done using the CRNS surface soil moisture time series based on the standard transfer function as well as on the UTS. Lastly, we test whether the estimation of the representative measurement depth of CRNS and thus, the depth of the first soil layer, has an influence on the resulting modelled soil moisture time series in the second layer. An overview of the different applications of the SMAR model performed in this study is given in Fig. 2.

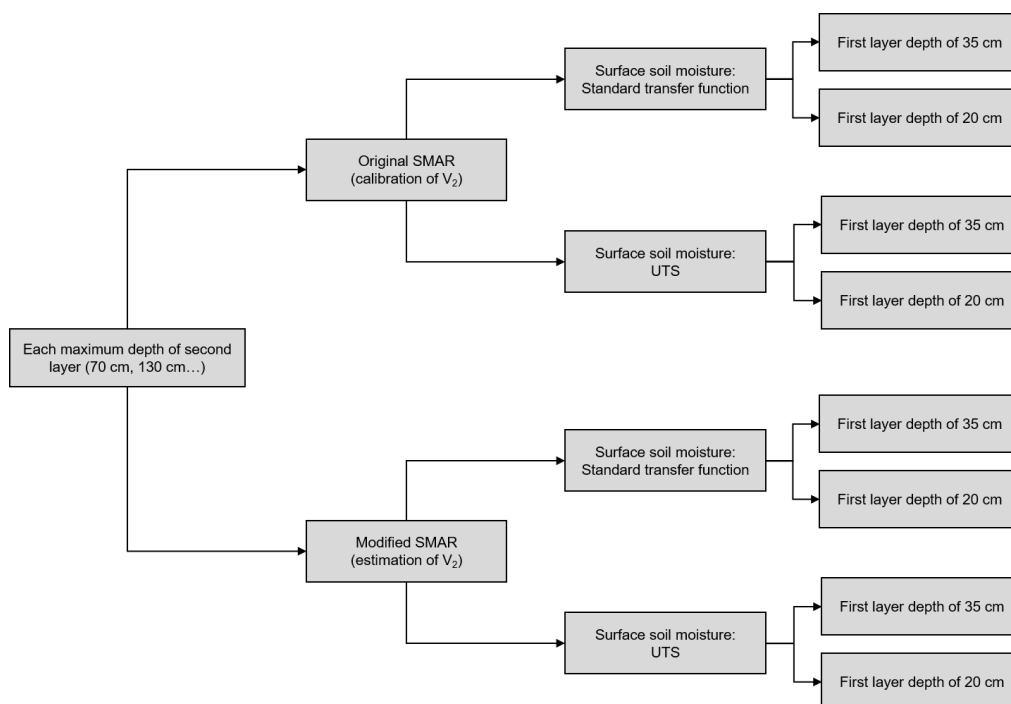


Figure 2. Overview of SMAR models set up in the scope of this study to compare the original SMAR based on the calibration of the water loss V_2 and the modified SMAR which does not require calibration.

To assess the robustness of the modified and uncalibrated SMAR model, we made a simple assessment of parameter uncertainty and its effect on the model results. We set up an ensemble of 50 realizations of the modified SMAR by randomly varying the values for n_1 , n_2 , sc_1 , sc_2 , sw_2 and R_1 in a range of $\pm 10\%$. These sensitivity runs of the modified, uncalibrated SMAR are then assessed using the minimum to maximum range of calculated root mean square error (RMSE) between the simulated soil moisture time series in the second soil layer and the reference from in-situ sensors. In satellite soil moisture estimations, a threshold of $0.06 \text{ cm}^3 \text{ cm}^{-3}$ has been used (Jackson et al., 2010) to evaluate the original SMAR performance for



root-zone soil moisture estimates based on satellite-derived surface soil moisture information (Baldwin et al., 2019). We adopt this benchmark for evaluating the performance of the uncalibrated, modified SMAR in this study.

305 Lastly, we performed a full calibration of the original and modified SMAR models in order to estimate the best possible simulation results within a physically acceptable range of the model parameters. This was done by randomly varying the values for n_1 , n_2 , sc_1 , sc_2 , sw_2 and R_1 in a range of $\pm 20\%$. For the original SMAR model, the water loss term V_2 was calibrated instead of the R_1 with values in the range between 1 and a maximum of 500 mm. The calibration was performed by selecting the parameter combination that resulted in the lowest RMSE among a total of 10,000 random parameter sets. For 310 the full calibration scenarios, we defined the year 2017 as the calibration period, while the entire study period (2016-2022) is used to evaluate the depth-extrapolated soil moisture time series. Except for the fact that several parameters were calibrated, the different scenarios are identical to those where just the V_2 parameter was calibrated (see Fig. 2). In all SMAR applications in this study, the initial soil moisture content of the second layer was set to the first CRNS-derived soil moisture record of the first layer. The SMAR model with physically reasonable environmental value ranges showed generally low performance 315 as described in the results section and led to some additional calibration tests of the model. Experimental calibration runs indicated that calibration parameters in a non-physical value range could produce better model results. Therefore, a second full calibration was performed where the values of the parameters sc_1 , sc_2 and sw_2 were allowed to range from -1 to their initial, literature-based value while the range for other model parameters remained unchanged.

The SMAR model was originally designed to depth-extrapolate surface soil moisture time series on a daily resolution, as 320 it assumes that all water above field capacity sc_1 infiltrates into the second layer within one day (Manfreda et al., 2014). Consequently, the SMAR model has been applied on a daily resolution in previous studies (e.g., Baldwin et al., 2017, 2019). In CRNS research, an hourly temporal resolution is the community standard and therefore, we test whether the SMAR models in their original and modified forms can also be applied at hourly resolution with a reasonable goodness-of-fit. All analyses described in this chapter are therefore carried out on both a daily and hourly basis.

325 All calculations were performed in R statistical software (R Core Team, 2018, 2023) using the hydroGOF package (Zambrano-Bigiarini, 2017, 2020) for calculating goodness-of-fit measures which evaluate absolute values and time series dynamics, namely the RMSE, the Kling-Gupta-Efficiency (KGE) (Gupta et al., 2009) as well as the Pearson correlation coefficient.

3 Results and discussion

3.1 CRNS-derived surface soil moisture time series

330 The goodness-of-fit of the calibrated CRNS-based soil moisture time series to the time series derived from in-situ point observations is shown for the two transfer functions Tab. 2. When the different transfer functions are calibrated against an arithmetic average soil moisture from soil samples and compared to an arithmetic average of soil moisture time series in 10-30 cm depth, the Pearson correlation coefficient and the KGE are lower than when using a weighted average of soil moisture observations for calibration as proposed by Köhli et al. (2015) and Schrön et al. (2017). However, the RMSE is slightly higher for the calibration 335 against the weighted observations. This might be linked to differences between the laboratory measurements of soil moisture



in the soil samples (which were used for calibration) and the continuous soil moisture data obtained from the in-situ sensors. Overall, however, in view of the much better KGE and correlation values, the results underline the importance of the weighting procedures when calibrating the CRNS observations to derive soil moisture estimates or comparing them to observations from in-situ soil moisture sensors.

Table 2. Goodness-of-fit between the CRNS-derived soil moisture time series and the arithmetic and weighted average soil moisture time series from the local in-situ point-sale soil moisture sensors in 10-30 cm depth. The different neutron to soil moisture transfer functions are independently calibrated against soil moisture from soil samples taken in February 2019. The UTS transfer function can be used with different parameter sets originating from different neutron transport models which are either based on an energy level threshold (thl) or a more realistic detector response functions (drf).

| Transfer function | In-situ soil moisture | Calibration parameter [cph] | KGE [-] | RMSE [$\text{cm}^3 \text{cm}^{-3}$] | Pearson correlation [-] |
|-------------------|-----------------------|-----------------------------|---------|---------------------------------------|-------------------------|
| Revised standard | | 777 | 0.08 | 0.030 | 0.88 |
| UTS URANOS drf | | 1245 | 0.14 | 0.029 | 0.86 |
| UTS URANOS thl | Arithmetic average | 1596 | 0.59 | 0.020 | 0.87 |
| UTS MCNP drf | | 1294 | 0.33 | 0.025 | 0.87 |
| UTS MCNP thl | | 1645 | 0.59 | 0.021 | 0.87 |
| Revised standard | | 809 | 0.46 | 0.030 | 0.91 |
| UTS URANOS drf | | 1302 | 0.49 | 0.029 | 0.89 |
| UTS URANOS thl | Weighted average | 1693 | 0.81 | 0.022 | 0.90 |
| UTS MCNP drf | | 1357 | 0.60 | 0.027 | 0.90 |
| UTS MCNP thl | | 1741 | 0.77 | 0.023 | 0.90 |

340 The goodness-of-fit of the CRNS-derived soil moisture time series that are based on the revised standard transfer function is always lower than for those that are derived with the UTS all parameters sets, especially when the KGE is considered, showing the improved soil moisture estimation with the UTS. However, the parameters sets of the UTS mimicking the varying sensitivity of a real neutron detector to neutrons of different energies (URANOS drf, MCNP drf) perform worse than those which rely on a simple energy range threshold (URANOS thl, MCNP thl). This counter-intuitive result has been previously described by
 345 Köhli et al. (2021) and could be related to the high sensitivity of the CRNS method to the soil moisture dynamics in the first few centimetres of the soil where unfortunately no in-situ sensors are installed (the uppermost sensors are installed in 10 cm depth). Therefore, the better performance of the energy threshold parameters sets of the UTS can be related to insufficient reference soil moisture information from the in-situ sensor network. Generally, the UTS with the parameter sets representing the response of a real neutron detector can be expected to provide more accurate results. Here, the UTS with parameter set
 350 MNCP drf reveals a higher statistical goodness-of-fit compared to the URANOS drf parameter set which is in line with the findings presented in Köhli et al. (2021). The improved performance of the UTS with the parameter set MNCP drf compared



to the standard transfer function is shown in Fig. 3, revealing that the latter tends to overestimate soil moisture under the wet winter conditions and underestimate soil moisture under dry summer conditions.

355 Different from the study of Köhli et al. (2021) which introduced the UTS, we apply UTS to derive soil moisture from neutron observations at a forest site. The UTS calibration parameter N_D represents the average count rate under boundary conditions of the neutron transport simulations conducted to derive the UTS. Therefore, N_D can be expected to be close to the average corrected neutron intensity observed at a study site with little or without vegetation or other above-ground hydrogen pools influencing the observed neutron intensity. At our study site, the calibrated N_D is much higher than the observed average corrected neutron intensity N_{pi} (557 cph). This is probably caused by the influence of the forest vegetation on observed neutron
360 intensities and the calibration parameter of the transfer function and has been similarly described for the standard transfer function by Baatz et al. (2015). As hydrogen stored in air humidity influences the functional relationship between neutron intensities and soil moisture, hydrogen stored in vegetation might have a similar effect. Therefore, a correction or inclusion approach for other above-ground hydrogen pools such as vegetation may yield an even better performance of the UTS and may be investigated in future studies.

365 Our analyses confirm the improved performance of the UTS compared to the standard transfer function. In order to test whether the improved performance in deriving surface soil moisture translates into a better estimation of soil moisture in deeper layers, we apply the SMAR model using the surface soil moisture time series based on both the revised standard transfer function and the UTS with the MCNP drf parameter set (Fig. 3).

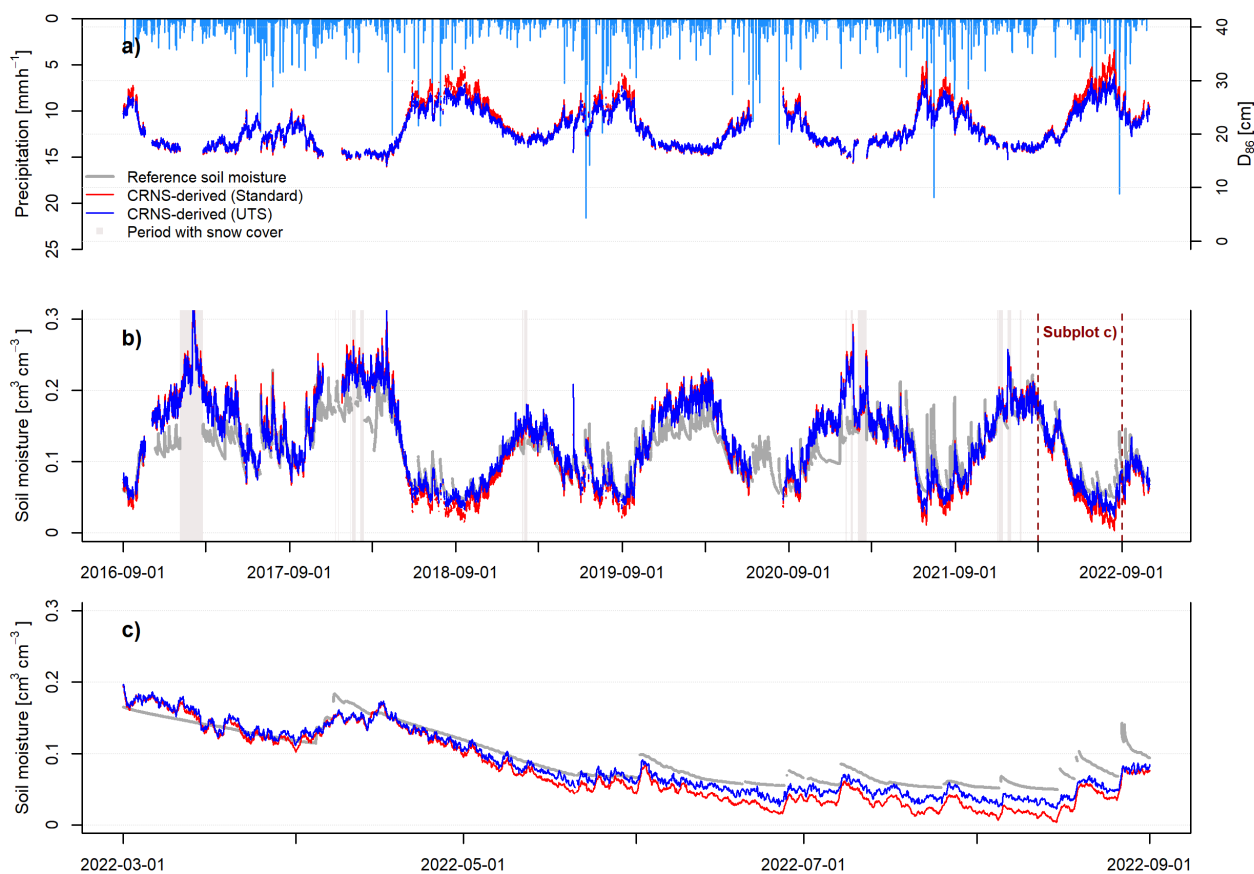


Figure 3. Soil moisture estimates with CRNS. (a) estimated time-variable sensitive measurement depth D_{86} of the CRNS-approach and precipitation time series (light blue bars); (b) soil moisture time series derived with the revised standard transfer function and the UTS with parameter set MCNP drf and (c) a period in 2022 illustrating the differences between the two CRNS-derived soil moisture time series.



3.2 Depth-extrapolation of CRNS-derived soil moisture time series

370 3.2.1 Original SMAR with calibrated water loss and uncalibrated, modified SMAR

The performance measures and the corresponding values for the depth-extrapolated soil moisture time series based on the calibrated original SMAR (calibrated water loss only) and the uncalibrated modified SMAR (estimated water loss based on eq. (11-14)) are listed in Tab. 3 as well as Tab. 4 and exemplary time series for a second layer depth of 130 cm are shown in Fig. 4 and Fig. 5 for a hourly and daily resolution, respectively. The standard transfer function and the UTS produce similar
375 results with RMSE values ranging between 0.055 and 0.015 $\text{cm}^3 \text{cm}^{-3}$ for hourly values and between 0.054 and 0.014 $\text{cm}^3 \text{cm}^{-3}$ for daily values over all simulated scenarios. The SMAR model with daily resolution generally results in a higher goodness-of-fit. The correlation coefficients tend to be lower for the scenarios using the uncalibrated, modified SMAR and higher for the original SMAR with calibrated water loss. For KGE, the results are the opposite.

The better performance at a daily time step (irrespective of the depth-extrapolation method) can be attributed to the fact that
380 it is generally assumed that all water above field capacity infiltrates from the first into the second layer within one time step. While this may be a reasonable assumption on a daily time step for which the SMAR model was designed for (Manfreda et al., 2014), this prerequisite is likely to be violated at the hourly time step. Nevertheless, for our study site, the differences in terms of the RMSE are rather small, indicating that the SMAR model may also be used with an hourly resolution.

Following the RMSE threshold of $\leq 0.06 \text{ cm}^3 \text{cm}^{-3}$ which has been used to evaluate the original SMAR performance
385 (Baldwin et al., 2019; Guo et al., 2023), all simulations with the original and with the modified SMAR and both with an hourly and daily resolution lie below this threshold. This indicates that all SMAR models result in acceptable soil moisture time series for the second soil layer down to 450 cm depth according to RMSE performance. However, taking the dynamic goodness-of-fit parameters KGE and correlation coefficient into account, the performance with regard to the temporal dynamics is not satisfactory. This can also be visually identified from Fig. 4 and Fig. 5 for a second layer depth of 130 cm. The original SMAR
390 with calibrated constant water loss reaches the wilting point of the second soil layer over large parts of the study period, indicating that the water loss calibrated by minimizing RMSE, results in a high constant water loss to match the reference average water content of the second layer but thereby causing too strong and rapid decreases of soil moisture in dry summer periods. Here, the uncalibrated, modified SMAR model provides more realistic gradual decreases of soil moisture, leading to a better performance when visually assessing the time series. This is also true for the maximum second layer depth of 450 cm
395 investigated in this study (Fig. A1 and Fig. A2) and illustrates that care should be taken when relying on statistical goodness-of-fit measures and that a visual assessment and interpretation of the simulation results should be undertaken. Nevertheless, it should be noted that the simulated soil moisture time series both for the original and for the modified SMAR do not represent intermediate pulses of increased soil moisture seen in the reference data even during the drier summer period.

For large maximum depths of the second layer such as 450 cm, the original SMAR with calibrated water loss better simulates
400 the amplitudes of soil moisture in the second layer for a temporal resolution of both hours and days. This indicates that the water loss estimated with the modified SMAR is too low for large depths. The condition of eq. (13), imposing that no evapotranspiration losses occur when water percolates from the first to the second layer, could be one reason. Another reason



could be uncertainties of the relative root fraction that is required to scale the water losses from the the first to the second layer. The use of an exponential model to describe the cumulative root distribution, as done in this study, is highly simplistic and such
405 models generally remain under debate (e.g. Pierret et al., 2016). Furthermore, too much water percolating from the first into the second soil layer may be compensated through the calibration of the water loss parameter in the original SMAR model, but this cannot be done when the uncalibrated, modified SMAR is applied.

Another major reason for the generally poor performance of both the original and the modified SMAR can be the literature-based soil physical parameters used here in order to apply the SMAR model without calibration against in-situ reference
410 measurements. In ensemble simulations with the modified SMAR, the soil physical parameters were varied in a range of $\pm 10\%$. The minimum and maximum RMSE values derived from the 50 hourly and daily ensemble runs are shown in Tab. A1. It can be seen that smaller RMSE values can be achieved with parameter values that are different from the initial ones (Tab. 3). The maximum RMSE for all depths except for 70 cm still meet the RMSE benchmark criterion, indicating a certain robustness of the uncalibrated, modified SMAR model presented in this study if the soil physical parameters can be reasonable well
415 estimated.

We also tested the impact of the input surface soil moisture time series to both the original SMAR with calibrated water loss and the uncalibrated, modified SMAR. Using either the CRNS-derived soil moisture time series based on the UTS equation or the revised standard equation for the first layer results in visually similar results with similar RMSE values, slightly higher correlation coefficients for the second case, and slightly better KGE values for the first case (Tab. 3, Tab. 4). Overall, in this
420 study, a better estimated surface soil moisture time series from CRNS does not necessarily translate into a distinct improvement of the depth-extrapolated time series. This may be explained by the considerable overall deficiencies of the SMAR models to represent the soil moisture dynamics at our study site which are larger than the differences between the surface soil moisture time series derived with the different neutron-to-soil moisture transfer functions.

In contrast, improvements of the depth-extrapolated soil moisture times series in the second layer can be seen when the depth
425 of the top soil layer in the SMAR model is taken to be the median calculated sensitive measurement depth (D_{86} , Schrön et al. (2017)) of the CRNS technique. Here, the statistical goodness-of-fit is generally higher compared to using an assumed sensitive depth of 35 cm for the top soil layer. This is the case for both the standard and the modified SMAR model and independent of the transfer function used for the CRNS soil moisture in the top layer (standard or UTS) with hourly and daily resolution. The better matching time series compared to the reference time series is also visible in Fig. 4 and Fig. 5 and is expressed through
430 the RMSE values in Tab. 3 and Tab. 4. The nature of the SMAR model as a water balance approach implies that the correct estimation of the volume of the upper soil layer and its storage is directly related to the accuracy of the depth-extrapolated time series of the second soil layer. Consequently, an accurate assessment of the sensitive measurement depth of CRNS is also highly important when using CRNS-derived soil moisture time series in e.g. (soil) hydrological model applications.



Table 3. Statistical goodness-of-fit between the depth-extrapolated *hourly* soil moisture time series from CRNS surface observations and the average soil moisture time series in the second layer calculated from the available in-situ point-scale soil moisture sensors. The water loss parameter is either a calibrated static value (original SMAR model) or estimated based on the procedure described for the modified SMAR model, see chapter 2.

| Layer 2 depth [cm] | Layer 1 depth [cm] | Transfer function | SMAR | Water loss | V_2 [mm h ⁻¹] | RMSE [cm ³ cm ⁻³] | Pearson correlation | KGE [-] |
|--------------------|--------------------|-------------------|------------|------------|-----------------------------|--|---------------------|---------|
| 70 | 35 | Revised standard | Modified | Estimated | - | 0.055 | 0.735 | -1.74 |
| | | | Original | Calibrated | 156 | 0.04 | 0.589 | 0.13 |
| | UTS MCNP drf | Modified | Estimated | - | 0.053 | 0.733 | -1.64 | |
| | | Original | Calibrated | 132 | 0.041 | 0.577 | 0.14 | |
| | 20 | Revised standard | Modified | Estimated | - | 0.041 | 0.803 | -1.54 |
| | | | Original | Calibrated | 64 | 0.035 | 0.661 | 0.24 |
| UTS MCNP drf | Modified | Estimated | - | 0.040 | 0.795 | -1.44 | | |
| | Original | Calibrated | 58 | 0.035 | 0.654 | -0.24 | | |
| 130 | 35 | Revised standard | Modified | Estimated | - | 0.036 | 0.711 | -0.85 |
| | | | Original | Calibrated | 104 | 0.041 | 0.537 | 0.12 |
| | UTS MCNP drf | Modified | Estimated | - | 0.035 | 0.714 | -0.83 | |
| | | Original | Calibrated | 94 | 0.041 | 0.529 | 0.13 | |
| | 20 | Revised standard | Modified | Estimated | - | 0.033 | 0.773 | -0.81 |
| | | | Original | Calibrated | 58 | 0.038 | 0.608 | 0.16 |
| UTS MCNP drf | Modified | Estimated | - | 0.033 | 0.768 | -0.79 | | |
| | Original | Calibrated | 52 | 0.038 | 0.604 | 0.17 | | |
| 200 | 35 | Revised standard | Modified | Estimated | - | 0.033 | 0.698 | -0.82 |
| | | | Original | Calibrated | 113 | 0.036 | 0.492 | 0.15 |
| | UTS MCNP drf | Modified | Estimated | - | 0.032 | 0.704 | -0.81 | |
| | | Original | Calibrated | 102 | 0.036 | 0.489 | 0.15 | |
| | 20 | Revised standard | Modified | Estimated | - | 0.032 | 0.743 | -0.78 |
| | | | Original | Calibrated | 63 | 0.034 | 0.557 | 0.18 |
| UTS MCNP drf | Modified | Estimated | - | 0.031 | 0.741 | -0.77 | | |
| | Original | Calibrated | 57 | 0.034 | 0.556 | 0.19 | | |
| 300 | 35 | Revised standard | Modified | Estimated | - | 0.036 | 0.676 | -1.36 |
| | | | Original | Calibrated | 157 | 0.026 | 0.450 | 0.25 |
| | UTS MCNP drf | Modified | Estimated | - | 0.035 | 0.681 | -1.33 | |
| | | Original | Calibrated | 142 | 0.026 | 0.449 | 0.25 | |
| | 20 | Revised standard | Modified | Estimated | - | 0.034 | 0.698 | -1.27 |
| | | | Original | Calibrated | 87 | 0.025 | 0.511 | 0.29 |
| UTS MCNP drf | Modified | Estimated | - | 0.033 | 0.694 | -1.24 | | |
| | Original | Calibrated | 79 | 0.025 | 0.512 | 0.29 | | |
| 450 | 35 | Revised standard | Modified | Estimated | - | 0.044 | 0.545 | -2.02 |
| | | | Original | Calibrated | 300 | 0.015 | 0.333 | 0.3 |
| | UTS MCNP drf | Modified | Estimated | - | 0.043 | 0.556 | -1.98 | |
| | | Original | Calibrated | 269 | 0.015 | 0.336 | 0.31 | |
| | 20 | Revised standard | Modified | Estimated | - | 0.040 | 0.558 | -1.91 |
| | | | Original | Calibrated | 158 | 0.015 | 0.392 | 0.33 |
| UTS MCNP drf | Modified | Estimated | - | 0.039 | 0.566 | -1.88 | | |
| | Original | Calibrated | 143 | 0.015 | 0.396 | 0.33 | | |

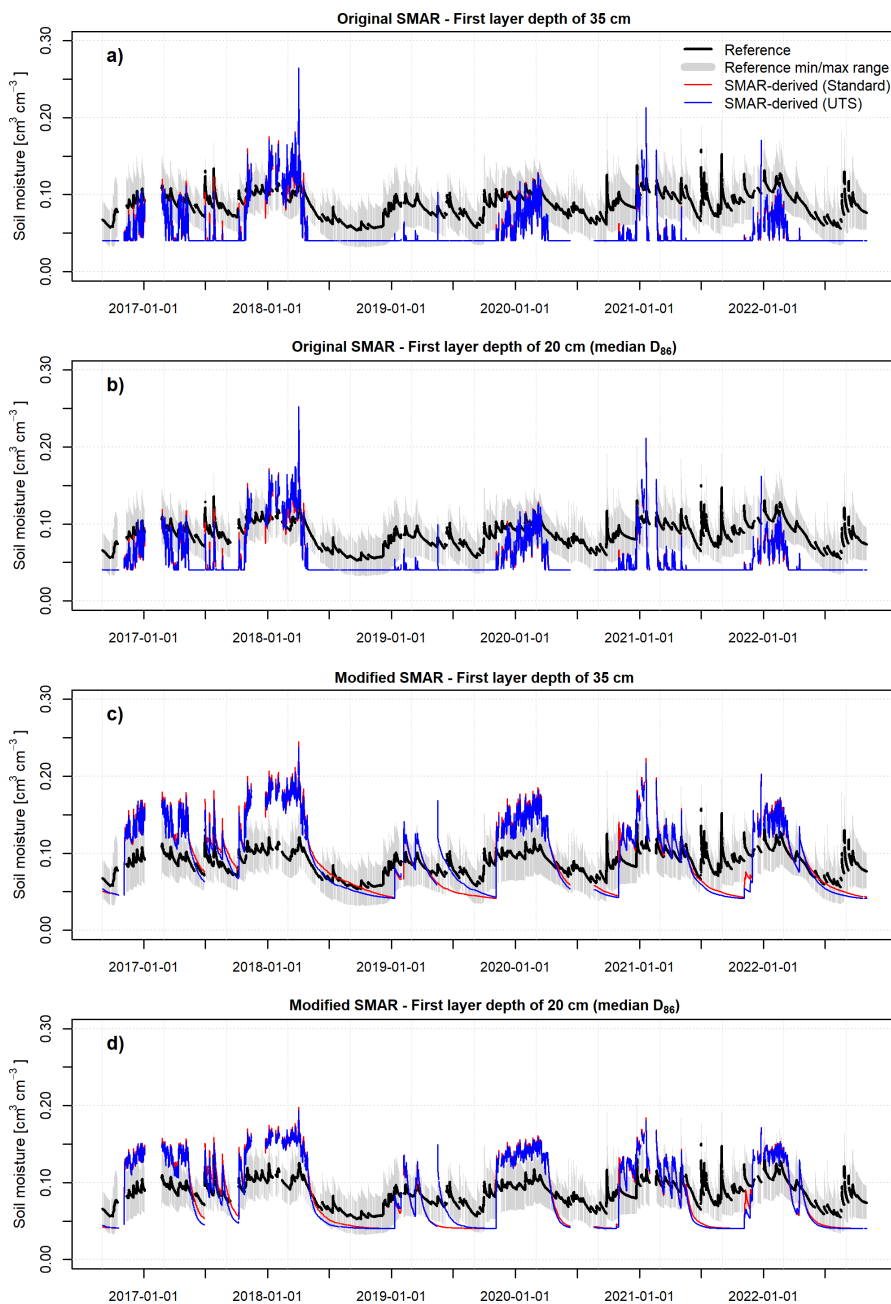


Figure 4. Hourly depth-extrapolated soil moisture time series for a depth of 130 cm using the calibrated standard SMAR model (calibrated water loss V_2) with a top layer depth of 35 cm (a), and 20 cm (b) as well as the depth-extrapolated soil moisture time series based on the uncalibrated modified SMAR (estimated water loss) model presented in this study (top layer depth of 35 cm (c) and 20 cm (d)) based on the CRNS-derived surface soil moisture time series from the standard transfer function and the UTS.



Table 4. Statistical goodness-of-fit between the depth-extrapolated *daily* surface soil moisture time from CRNS and the average soil moisture time series in the second layer calculated from the available in-situ point-scale soil moisture sensors. The water loss parameter is either as a calibrated static value (original SMAR model) or estimated based on the procedure described in the methods section (modified SMAR model, see chapter 2).

| Layer 2 depth [cm] | Layer 1 depth [cm] | Transfer function | SMAR | Water loss | V_2 [mm h ⁻¹] | RMSE [cm ³ cm ⁻³] | Pearson correlation | KGGE [-] |
|--------------------|--------------------|-------------------|------------|------------|-----------------------------|--|---------------------|----------|
| 70 | 35 | Revised standard | Modified | Estimated | - | 0.054 | 0.685 | -1.18 |
| | | | Original | Calibrated | 131 | 0.04 | 0.602 | 0.1 |
| | UTS MCNP drf | Modified | Estimated | - | 0.051 | 0.675 | -0.92 | |
| | | Original | Calibrated | 113 | 0.04 | 0.59 | 0.11 | |
| | 20 | Revised standard | Modified | Estimated | - | 0.037 | 0.76 | -1.03 |
| | | | Original | Calibrated | 56 | 0.034 | 0.688 | 0.2 |
| UTS MCNP drf | Modified | Estimated | - | 0.035 | 0.752 | -0.78 | | |
| | Original | Calibrated | 51 | 0.034 | 0.678 | 0.22 | | |
| 130 | 35 | Revised standard | Modified | Estimated | - | 0.034 | 0.626 | -0.38 |
| | | | Original | Calibrated | 87 | 0.039 | 0.575 | 0.08 |
| | UTS MCNP drf | Modified | Estimated | - | 0.032 | 0.614 | -0.22 | |
| | | Original | Calibrated | 79 | 0.04 | 0.564 | 0.09 | |
| | 20 | Revised standard | Modified | Estimated | - | 0.029 | 0.697 | -0.35 |
| | | | Original | Calibrated | 48 | 0.036 | 0.644 | 0.12 |
| UTS MCNP drf | Modified | Estimated | - | 0.028 | 0.68 | -0.19 | | |
| | Original | Calibrated | 44 | 0.036 | 0.635 | 0.13 | | |
| 200 | 35 | Revised standard | Modified | Estimated | - | 0.031 | 0.619 | -0.34 |
| | | | Original | Calibrated | 91 | 0.035 | 0.546 | 0.09 |
| | UTS MCNP drf | Modified | Estimated | - | 0.03 | 0.608 | -0.19 | |
| | | Original | Calibrated | 83 | 0.035 | 0.538 | 0.1 | |
| | 20 | Revised standard | Modified | Estimated | - | 0.027 | 0.685 | -0.3 |
| | | | Original | Calibrated | 51 | 0.032 | 0.611 | 0.13 |
| UTS MCNP drf | Modified | Estimated | - | 0.026 | 0.668 | -0.16 | | |
| | Original | Calibrated | 47 | 0.032 | 0.605 | 0.13 | | |
| 300 | 35 | Revised standard | Modified | Estimated | - | 0.035 | 0.633 | -0.72 |
| | | | Original | Calibrated | 124 | 0.024 | 0.515 | 0.2 |
| | UTS MCNP drf | Modified | Estimated | - | 0.034 | 0.625 | -0.56 | |
| | | Original | Calibrated | 113 | 0.025 | 0.511 | 0.2 | |
| | 20 | Revised standard | Modified | Estimated | - | 0.027 | 0.688 | -0.64 |
| | | | Original | Calibrated | 67 | 0.023 | 0.587 | 0.25 |
| UTS MCNP drf | Modified | Estimated | - | 0.027 | 0.673 | -0.48 | | |
| | Original | Calibrated | 62 | 0.023 | 0.583 | 0.25 | | |
| 450 | 35 | Revised standard | Modified | Estimated | - | 0.043 | 0.551 | -1.18 |
| | | | Original | Calibrated | 237 | 0.014 | 0.392 | 0.37 |
| | UTS MCNP drf | Modified | Estimated | - | 0.043 | 0.549 | -1.03 | |
| | | Original | Calibrated | 215 | 0.014 | 0.392 | 0.37 | |
| | 20 | Revised standard | Modified | Estimated | - | 0.032 | 0.594 | -1.1 |
| | | | Original | Calibrated | 122 | 0.014 | 0.47 | 0.39 |
| UTS MCNP drf | Modified | Estimated | - | 0.032 | 0.581 | -0.95 | | |
| | Original | Calibrated | 112 | 0.014 | 0.47 | 0.39 | | |

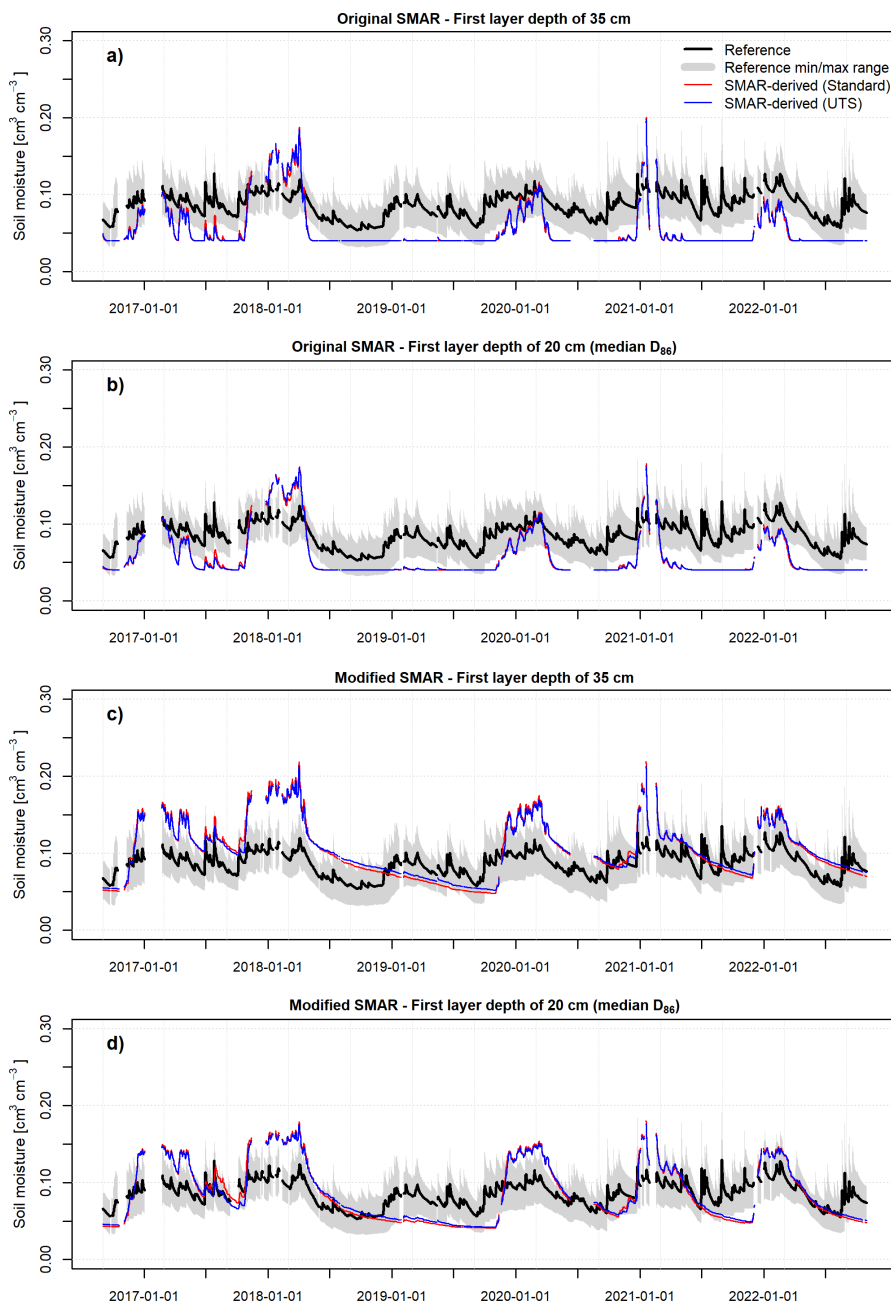


Figure 5. Daily depth-extrapolated soil moisture time series for a depth of 130 cm using the calibrated standard SMAR model (calibrated water loss V_2) with a top layer depth of 35 cm (a), and 20 cm (b) as well as the depth-extrapolated soil moisture time series based on the uncalibrated modified SMAR (estimated water loss) model presented in this study (top layer depth of 35 cm (c) and 20 cm (d)) based on the CRNS-derived surface soil moisture time series from the standard transfer function and the UTS.



3.2.2 Full calibration of the original and modified SMAR

435 To further assess the performance of the original and modified SMAR at the study site, we performed a full (all parameter)
calibration of the two SMAR models with 10,000 random combinations of the soil physical parameters. The initially assigned
soil physical parameters were altered in the range of $\pm 20\%$ to assign values in a physically acceptable range for the sandy
soils at the study site. Additionally to the soil physical parameters, the bulk water loss V_2 in the original SMAR was calibrated
with random values in the range from 1 to 500 mm. For the modified SMAR model, the relative root fraction in the first layer
440 R_l was varied in the range of $\pm 20\%$ instead.

The results of the full calibration can be found in Tab. 5 and Tab. 6 and exemplary time series for a second layer depth of
130 cm are shown in Fig. 6 and Fig. 7 for a hourly and daily resolution, respectively. The results for the maximum depth of
450 450 cm can be found in the appendix. As expected, minimizing the RMSE in the calibration period 2017 leads to a decrease of
the RMSE for the entire study period compared to the uncalibrated modified SMAR or when calibrating the water loss term
in the original SMAR only. This is the case for both the hourly and daily time step, with generally better performance for the
latter in terms of RMSE and KGE. Using a first layer depth of 20 cm instead of 35 cm leads to better soil moisture dynamics
in the deeper layers. This is in line with results presented in the previous chapters when comparing the uncalibrated, modified
SMAR and the original SMAR with calibrated water loss.

Following the statistical goodness-of-fit parameters in Tab. 5 and Tab. 6, the modified SMAR performs worse than the
450 calibrated original SMAR in different depths after all parameters have been calibrated. This may be attributed to using a
single-objective optimization for minimizing the RMSE, only. Furthermore, in the original SMAR, the bulk water loss from
the second layer was optimized while for the modified SMAR, only the cumulative root fraction in the first layer was adjusted.
This leads to more restricted conditions for the modified SMAR model. For example, calibrating the estimated complete water
loss in the latter eq. 11 based on a calibration factor could lead to improved the results of the fully calibrated, modified SMAR
455 and more close to those derived for the fully calibrated original SMAR. Nevertheless, the generally higher process restrictions
due to the defined estimation of ET_2 and P_2 in eq. 13–14 of the modified SMAR remain.

In summary, the full calibration of the original and modified SMAR model with soil model parameters in physically rea-
sonable value range show similar characteristics to those scenarios described in the previous chapter where literature-based
values were assigned for soil physical parameters and only the bulk water loss V_2 was calibrated. Although the overall vi-
460 sual performance improved and a higher statistical goodness-of-fit can be achieved when all environmental model parameters
are calibrated, the original and modified SMAR model tested in this study do not show satisfying results with respect to the
temporal dynamics of the soil moisture time series of the second layer. Many intermediate rainfall events are not captured and
thus, the reference soil moisture time series show a more dynamic behavior than those simulated by the original and modified
SMAR.

465 Calibration experiments revealed that assigning values in a non-physical parameter range, e.g., negative values, for soil
physical model parameters could lead to an improved performance of SMAR. When allowing a non-physical value range for
the model parameters sc_1 , sc_2 and sw_2 , the visual and statistical performance of both, the original and modified SMAR improve



dramatically with the exception of the depth of 70 cm. Again exemplary shown for a maximum depth of 130 and 450cm depth and both temporal resolutions, Fig. A5 – A8 as well as Tab. A2 – A3 illustrate the improved performance of both SMAR
470 models. The poor and even worse performance in the depth of 70 cm compared to the full calibration with physically reasonable values could be related to a non-sufficient value range for the calibrated parameters when values in a non-physically based value range are assigned. Even better results may also be derived for other depths with a different value range or by also calibrating the remaining parameters n_1 , n_2 , V_2 and R_f in a non-physically reasonable value range. These results show that satisfactory results with the original and the modified SMAR can be obtained at our study site at the expense of physical realism of the
475 model, and only if in-situ soil moisture measurements in the depth of interest are available for calibration.

3.2.3 General discussion

The evaluation of the original SMAR model against in-situ observations in previous studies showed a range of RMSE values and correlation coefficients (e.g., Manfreda et al., 2014; Faridani et al., 2017), indicating that the performance of the SMAR model varies between study sites.

480 The particular water flow dynamics at our study site located in a mixed forest with sandy soils may explain the overall unsatisfactory representation of soil moisture dynamics of the SMAR model when model parameters are assigned in a physically reasonable range. Preferential flow in macropores including bypass flow along roots (e.g., Nimmo, 2021) can result in highly conductive forest soils with infiltrating water being quickly transported from the surface to deeper layers. For example, Chandler et al. (2018) and Alaoui et al. (2011) found that forest soils can have higher saturated hydraulic conductivity compared
485 to other land cover types and combined with differing preferential flow processes this may lead to increased infiltration and percolation into lower layers of forest soils (e.g., Alaoui et al., 2011). Complex preferential flow and infiltration processes are unlikely to be properly captured by the SMAR as it allows water movement only for soil moisture conditions above field capacity. A more complex root distribution than the exponential one assumed in this study and related temporally varying transpiration water losses from different depths adds for complexity that is not captured by the SMAR model. Maysonnave et al.
490 (2022), for instance, found that root water uptake in forests can vary with time and depth depending on the water availability in different layers. These features can neither be reproduced by the original nor modified SMAR and makes forest sites generally challenging, in particular for simplified models. However, this may be partly compensated for when model-specific effective parameters are used. In this case, calibration against in-situ reference soil moisture information is required and the parameters lose their physical meaning and interpretability but may account for the particular soil hydraulic processes of the study site.

495 In addition to the simplicity of the model, the field-scale approach of this study adds further difficulties when evaluating the simulated soil moisture time series against point-scale soil moisture observations. The reason is their high spatio-temporal variability, especially in forests caused by e.g. heterogeneous evapotranspiration, interception, (e.g., Schume et al., 2003) and root distribution patterns (e.g., Jost et al., 2012). Even more, the decreasing number of reference in-situ soil moisture sensors with increasing soil depth may lead to a lower representativeness of the reference soil moisture time series at larger depths,
500 lowering comparability to the model results. Nevertheless, with point sensors down to 450 cm, this study allows for exploring the potential of SMAR for larger depths than usually feasible. Even when depths down to 450 cm are considered, the original



and modified SMAR meet the benchmark RMSE of $\leq 0.06 \text{ cm}^3 \text{ cm}^{-3}$ in scenarios with literature-based and with calibrated model parameters. This underlines the usefulness of SMAR to derive a first estimate of soil moisture in a second, deeper soil layer.

505 The largest limitation of the present study for evaluating the standard and the introduced modified SMAR models is its application to a single observation site. A comparison with other simple depth-extrapolation approaches including the soil water index (e.g., Wagner et al., 1999; Albergel et al., 2008), empirical approaches such as regression models (e.g., Zhang et al., 2017) and cumulative distribution function matching (e.g., Gao et al., 2018) as well as other versions of the SMAR model (e.g., Faridani et al., 2017) would allow for an improved evaluation of the presented modification of the SMAR model
510 and should be assessed in future studies at sites with a broader range of climatic conditions, vegetation covers and soils.



Table 5. Statistical goodness-of-fit between the depth-extrapolated *hourly* surface soil moisture time series from CRNS and the average soil moisture time series in the second layer calculated from the available in-situ point-scale soil moisture sensors with the fully calibrated SMAR in a physically acceptable parameter range. The calibrated model parameters and goodness-of-fit indicators for the original and modified SMAR model are shown.

| Layer 2 depth [cm] | Layer 1 depth [cm] | Transfer function | SMAR | n_1 [-] | n_2 [-] | sc_1 [$\text{cm}^3 \text{cm}^{-3}$] | sc_2 [$\text{cm}^3 \text{cm}^{-3}$] | sw_2 [$\text{cm}^3 \text{cm}^{-3}$] | V_2 [mm h^{-1}] | R_1 [-] | RMSE [$\text{cm}^3 \text{cm}^{-3}$] | Pearson correlation | KGE [-] |
|--------------------|--------------------|-------------------|----------|-----------|-----------|---|---|---|------------------------------|-----------|---------------------------------------|---------------------|---------|
| 70 | 35 | Revised standard | Modified | 0.56 | 0.34 | 0.19 | 0.10 | 0.04 | - | 0.77 | 0.030 | 0.584 | -0.286 |
| | | | Original | 0.50 | 0.36 | 0.13 | 0.11 | 0.05 | 377 | - | 0.029 | 0.709 | -0.029 |
| | | UTS MCNP drf | Modified | 0.59 | 0.33 | 0.19 | 0.10 | 0.04 | - | 0.78 | 0.027 | 0.587 | -0.148 |
| | Original | | 0.50 | 0.36 | 0.13 | 0.11 | 0.05 | 377 | - | 0.028 | 0.707 | 0.072 | |
| | 20 | Revised standard | Modified | 0.68 | 0.41 | 0.19 | 0.1 | 0.04 | - | 0.54 | 0.028 | 0.748 | -0.062 |
| | | | Original | 0.64 | 0.45 | 0.12 | 0.13 | 0.05 | 123 | - | 0.024 | 0.754 | 0.263 |
| UTS MCNP drf | | Modified | 0.67 | 0.42 | 0.18 | 0.10 | 0.05 | - | 0.54 | 0.025 | 0.736 | 0.041 | |
| | Original | 0.64 | 0.45 | 0.12 | 0.13 | 0.05 | 123 | - | 0.024 | 0.753 | 0.342 | | |
| 130 | 35 | Revised standard | Modified | 0.55 | 0.35 | 0.19 | 0.10 | 0.04 | - | 0.77 | 0.031 | 0.565 | -0.014 |
| | | | Original | 0.51 | 0.41 | 0.13 | 0.13 | 0.05 | 226 | - | 0.028 | 0.678 | 0.364 |
| | | UTS MCNP drf | Modified | 0.56 | 0.42 | 0.19 | 0.10 | 0.05 | - | 0.78 | 0.024 | 0.557 | 0.169 |
| | Original | | 0.57 | 0.36 | 0.13 | 0.10 | 0.05 | 136 | - | 0.028 | 0.681 | 0.093 | |
| | 20 | Revised standard | Modified | 0.63 | 0.45 | 0.18 | 0.10 | 0.05 | - | 0.53 | 0.026 | 0.692 | 0.175 |
| | | | Original | 0.64 | 0.45 | 0.12 | 0.13 | 0.05 | 123 | - | 0.026 | 0.724 | 0.372 |
| UTS MCNP drf | | Modified | 0.51 | 0.41 | 0.17 | 0.10 | 0.05 | - | 0.53 | 0.025 | 0.707 | 0.145 | |
| | Original | 0.64 | 0.45 | 0.12 | 0.13 | 0.05 | 123 | - | 0.026 | 0.727 | 0.438 | | |
| 200 | 35 | Revised standard | Modified | 0.54 | 0.33 | 0.19 | 0.1 | 0.04 | - | 0.74 | 0.026 | 0.576 | 0.113 |
| | | | Original | 0.51 | 0.41 | 0.13 | 0.13 | 0.05 | 226 | - | 0.025 | 0.634 | 0.378 |
| | | UTS MCNP drf | Modified | 0.60 | 0.40 | 0.19 | 0.10 | 0.04 | - | 0.77 | 0.023 | 0.574 | 0.164 |
| | Original | | 0.51 | 0.41 | 0.13 | 0.13 | 0.05 | 226 | - | 0.024 | 0.642 | 0.436 | |
| | 20 | Revised standard | Modified | 0.63 | 0.45 | 0.18 | 0.10 | 0.05 | - | 0.53 | 0.023 | 0.661 | 0.175 |
| | | | Original | 0.64 | 0.45 | 0.12 | 0.13 | 0.05 | 123 | - | 0.023 | 0.676 | 0.301 |
| UTS MCNP drf | | Modified | 0.51 | 0.41 | 0.17 | 0.10 | 0.05 | - | 0.52 | 0.023 | 0.682 | 0.135 | |
| | Original | 0.64 | 0.45 | 0.12 | 0.13 | 0.05 | 123 | - | 0.023 | 0.684 | 0.375 | | |
| 300 | 35 | Revised standard | Modified | 0.52 | 0.31 | 0.19 | 0.10 | 0.05 | - | 0.61 | 0.019 | 0.575 | -0.047 |
| | | | Original | 0.50 | 0.36 | 0.13 | 0.11 | 0.05 | 377 | - | 0.017 | 0.576 | 0.533 |
| | | UTS MCNP drf | Modified | 0.52 | 0.31 | 0.19 | 0.10 | 0.05 | - | 0.61 | 0.019 | 0.561 | 0.062 |
| | Original | | 0.51 | 0.45 | 0.13 | 0.14 | 0.05 | 370 | - | 0.016 | 0.585 | 0.523 | |
| | 20 | Revised standard | Modified | 0.63 | 0.31 | 0.19 | 0.10 | 0.05 | - | 0.43 | 0.020 | 0.591 | 0.059 |
| | | | Original | 0.76 | 0.42 | 0.13 | 0.14 | 0.05 | 230 | - | 0.016 | 0.617 | 0.576 |
| UTS MCNP drf | | Modified | 0.59 | 0.31 | 0.18 | 0.10 | 0.05 | - | 0.48 | 0.019 | 0.592 | 0.108 | |
| | Original | 0.68 | 0.36 | 0.12 | 0.10 | 0.05 | 136 | - | 0.015 | 0.629 | 0.512 | | |
| 450 | 35 | Revised standard | Modified | 0.51 | 0.32 | 0.19 | 0.10 | 0.04 | - | 0.59 | 0.023 | 0.425 | -0.851 |
| | | | Original | 0.52 | 0.31 | 0.17 | 0.11 | 0.05 | 482 | - | 0.011 | 0.287 | 0.075 |
| | | UTS MCNP drf | Modified | 0.52 | 0.31 | 0.19 | 0.10 | 0.05 | - | 0.61 | 0.018 | 0.451 | -0.234 |
| | Original | | 0.63 | 0.31 | 0.16 | 0.12 | 0.05 | 485 | - | 0.010 | 0.328 | 0.12 | |
| | 20 | Revised standard | Modified | 0.63 | 0.31 | 0.19 | 0.14 | 0.05 | - | 0.43 | 0.018 | 0.466 | -0.268 |
| | | | Original | 0.66 | 0.34 | 0.13 | 0.14 | 0.05 | 484 | - | 0.009 | 0.484 | 0.272 |
| UTS MCNP drf | | Modified | 0.63 | 0.31 | 0.19 | 0.10 | 0.05 | - | 0.43 | 0.017 | 0.461 | -0.145 | |
| | Original | 0.66 | 0.34 | 0.13 | 0.14 | 0.05 | 484 | - | 0.009 | 0.496 | 0.261 | | |

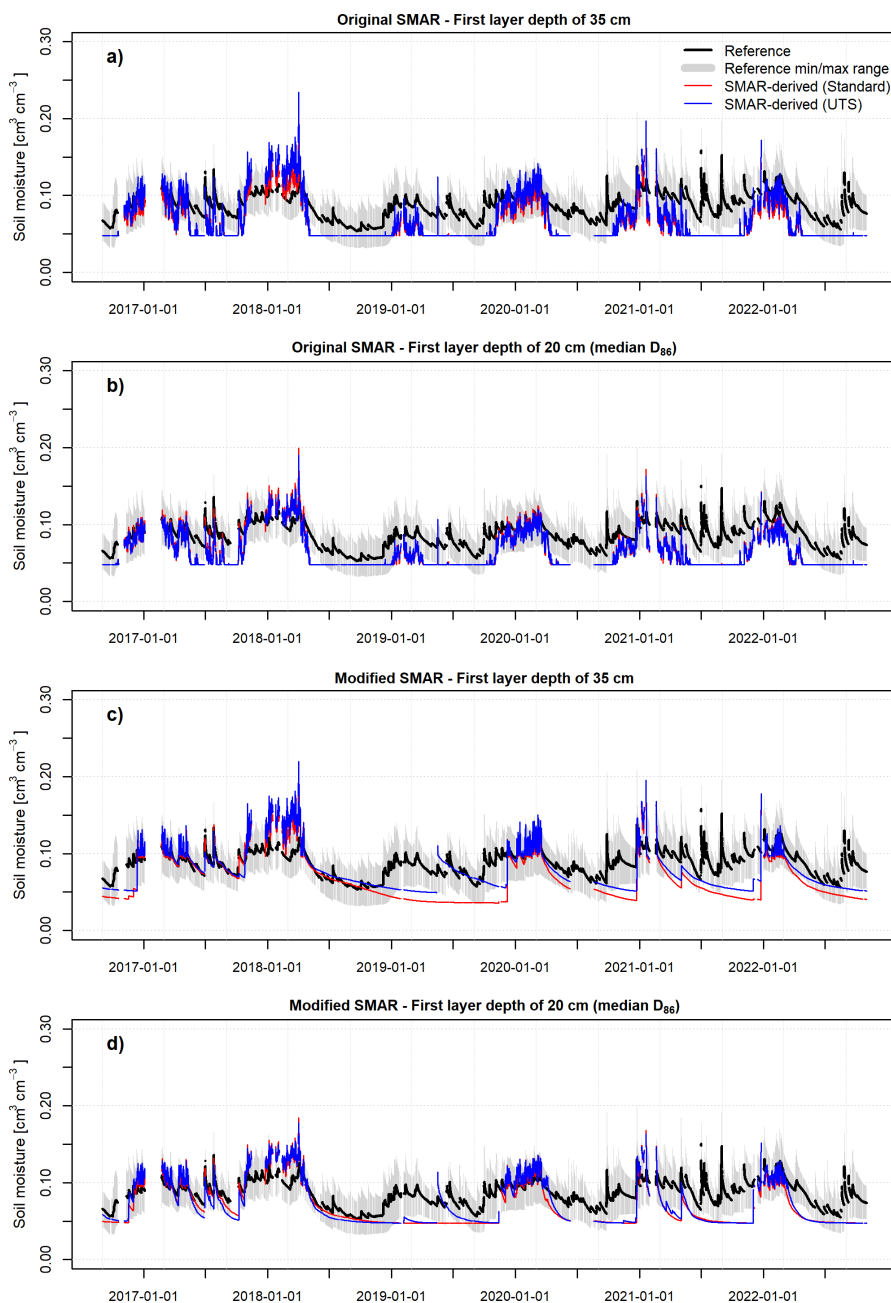


Figure 6. Hourly depth-extrapolated soil moisture time series for a depth of 130 cm using the standard SMAR model with a top layer depth of 35 cm (a), and 20 cm (b) as well as the depth-extrapolated soil moisture time series based on the modified SMAR model presented in this study (top layer depth of 35 cm (c) and 20 cm (d)) based on the CRNS-derived surface soil moisture time series from the standard transfer function and the UTS. The soil physical parameters n_1 , n_2 , sc_1 , sc_2 , sw_2 and R_1 were optimized by reducing the RMSE against reference soil moisture values in the year 2017. For the original SMAR model, the water loss term V_2 was calibrated instead of R_1 .



Table 6. Statistical goodness-of-fit between the depth-extrapolated *daily* surface soil moisture time from CRNS and the average soil moisture time series in the second layer calculated from the available in-situ point-scale soil moisture sensors with the fully calibrated SMAR in a physically acceptable parameter range. The calibrated model parameters and goodness-of-fit indicators for the original and modified SMAR model are shown.

| Layer 2 depth [cm] | Layer 1 depth [cm] | Transfer function | SMAR | n_1 [-] | n_2 [-] | sc_1 [$\text{cm}^3 \text{cm}^{-3}$] | sc_2 [$\text{cm}^3 \text{cm}^{-3}$] | sw_2 [$\text{cm}^3 \text{cm}^{-3}$] | V_2 [mm h^{-1}] | R_1 [-] | RMSE [$\text{cm}^3 \text{cm}^{-3}$] | Pearson correlation | KGE [-] | |
|--------------------|--------------------|-------------------|------------------|-----------|-----------|---|---|---|------------------------------|-----------|---------------------------------------|---------------------|---------|-------|
| 70 | 35 | Revised standard | Modified | 0.54 | 0.33 | 0.19 | 0.10 | 0.04 | - | 0.74 | 0.024 | 0.518 | 0.119 | |
| | | | Original | 0.50 | 0.36 | 0.13 | 0.11 | 0.05 | 377 | - | 0.029 | 0.710 | 0.011 | |
| | | UTS MCNP drf | Modified | 0.47 | 0.35 | 0.19 | 0.10 | 0.03 | - | 0.78 | 0.022 | 0.490 | 0.252 | |
| | | | Original | 0.50 | 0.36 | 0.13 | 0.11 | 0.05 | 377 | - | 0.028 | 0.707 | 0.111 | |
| | | 20 | Revised standard | Modified | 0.72 | 0.40 | 0.18 | 0.1 | 0.04 | - | 0.54 | 0.021 | 0.681 | 0.228 |
| | | | | Original | 0.64 | 0.45 | 0.12 | 0.13 | 0.05 | 123 | - | 0.024 | 0.766 | 0.316 |
| | UTS MCNP drf | Modified | 0.59 | 0.45 | 0.18 | 0.10 | 0.05 | - | 0.55 | 0.020 | 0.655 | 0.307 | | |
| | | Original | 0.64 | 0.45 | 0.12 | 0.13 | 0.05 | 123 | - | 0.023 | 0.763 | 0.389 | | |
| | 130 | 35 | Revised standard | Modified | 0.55 | 0.35 | 0.19 | 0.10 | 0.04 | - | 0.77 | 0.021 | 0.441 | 0.321 |
| | | | | Original | 0.57 | 0.36 | 0.13 | 0.10 | 0.05 | 136 | - | 0.028 | 0.694 | 0.086 |
| | | | UTS MCNP drf | Modified | 0.58 | 0.44 | 0.19 | 0.10 | 0.04 | - | 0.78 | 0.019 | 0.390 | 0.358 |
| | | | | Original | 0.57 | 0.36 | 0.13 | 0.10 | 0.05 | 136 | - | 0.028 | 0.694 | 0.176 |
| 20 | | | Revised standard | Modified | 0.59 | 0.45 | 0.18 | 0.10 | 0.05 | - | 0.55 | 0.021 | 0.585 | 0.351 |
| | | | | Original | 0.63 | 0.34 | 0.12 | 0.12 | 0.05 | 63 | - | 0.026 | 0.741 | 0.031 |
| UTS MCNP drf | | Modified | 0.55 | 0.33 | 0.15 | 0.10 | 0.04 | - | 0.54 | 0.022 | 0.689 | 0.165 | | |
| | | Original | 0.63 | 0.34 | 0.12 | 0.12 | 0.05 | 163 | - | 0.025 | 0.741 | 0.121 | | |
| 200 | | 35 | Revised standard | Modified | 0.54 | 0.33 | 0.19 | 0.10 | 0.04 | - | 0.74 | 0.019 | 0.425 | 0.334 |
| | | | | Original | 0.51 | 0.41 | 0.13 | 0.13 | 0.05 | 226 | - | 0.024 | 0.657 | 0.437 |
| | | | UTS MCNP drf | Modified | 0.45 | 0.44 | 0.19 | 0.10 | 0.04 | - | 0.75 | 0.018 | 0.321 | 0.304 |
| | | | | Original | 0.57 | 0.36 | 0.13 | 0.10 | 0.05 | 136 | - | 0.024 | 0.665 | 0.162 |
| | 20 | | Revised standard | Modified | 0.59 | 0.45 | 0.18 | 0.10 | 0.05 | - | 0.55 | 0.019 | 0.554 | 0.352 |
| | | | | Original | 0.64 | 0.45 | 0.12 | 0.13 | 0.05 | 123 | - | 0.022 | 0.705 | 0.390 |
| | UTS MCNP drf | Modified | 0.59 | 0.45 | 0.18 | 0.10 | 0.05 | - | 0.55 | 0.019 | 0.503 | 0.383 | | |
| | | Original | 0.64 | 0.45 | 0.12 | 0.13 | 0.05 | 123 | - | 0.022 | 0.708 | 0.448 | | |
| | 300 | 35 | Revised standard | Modified | 0.56 | 0.34 | 0.19 | 0.10 | 0.04 | - | 0.77 | 0.017 | 0.377 | 0.141 |
| | | | | Original | 0.53 | 0.44 | 0.13 | 0.11 | 0.05 | 323 | - | 0.016 | 0.605 | 0.504 |
| | | | UTS MCNP drf | Modified | 0.52 | 0.41 | 0.19 | 0.10 | 0.04 | - | 0.75 | 0.017 | 0.310 | 0.223 |
| | | | | Original | 0.53 | 0.44 | 0.13 | 0.11 | 0.05 | 323 | - | 0.016 | 0.610 | 0.538 |
| 20 | | | Revised standard | Modified | 0.68 | 0.41 | 0.19 | 0.10 | 0.04 | - | 0.54 | 0.018 | 0.446 | 0.171 |
| | | | | Original | 0.68 | 0.36 | 0.12 | 0.10 | 0.05 | 136 | - | 0.015 | 0.665 | 0.536 |
| UTS MCNP drf | | Modified | 0.52 | 0.41 | 0.18 | 0.11 | 0.05 | - | 0.54 | 0.017 | 0.376 | 0.178 | | |
| | | Original | 0.68 | 0.36 | 0.13 | 0.10 | 0.05 | 136 | - | 0.015 | 0.669 | 0.574 | | |
| 450 | | 35 | Revised standard | Modified | 0.52 | 0.31 | 0.19 | 0.10 | 0.05 | - | 0.61 | 0.016 | 0.362 | 0.05 |
| | | | | Original | 0.63 | 0.31 | 0.16 | 0.12 | 0.05 | 485 | - | 0.01 | 0.365 | 0.156 |
| | | | UTS MCNP drf | Modified | 0.52 | 0.31 | 0.19 | 0.10 | 0.05 | - | 0.61 | 0.016 | 0.291 | 0.028 |
| | | | | Original | 0.62 | 0.34 | 0.16 | 0.10 | 0.05 | 492 | - | 0.01 | 0.363 | 0.170 |
| | 20 | | Revised standard | Modified | 0.63 | 0.31 | 0.19 | 0.10 | 0.05 | - | 0.43 | 0.013 | 0.416 | 0.189 |
| | | | | Original | 0.66 | 0.34 | 0.13 | 0.14 | 0.05 | 484 | - | 0.009 | 0.517 | 0.283 |
| | UTS MCNP drf | Modified | 0.63 | 0.31 | 0.19 | 0.10 | 0.05 | - | 0.43 | 0.013 | 0.384 | 0.217 | | |
| | | Original | 0.66 | 0.34 | 0.13 | 0.14 | 0.05 | 484 | - | 0.009 | 0.527 | 0.270 | | |

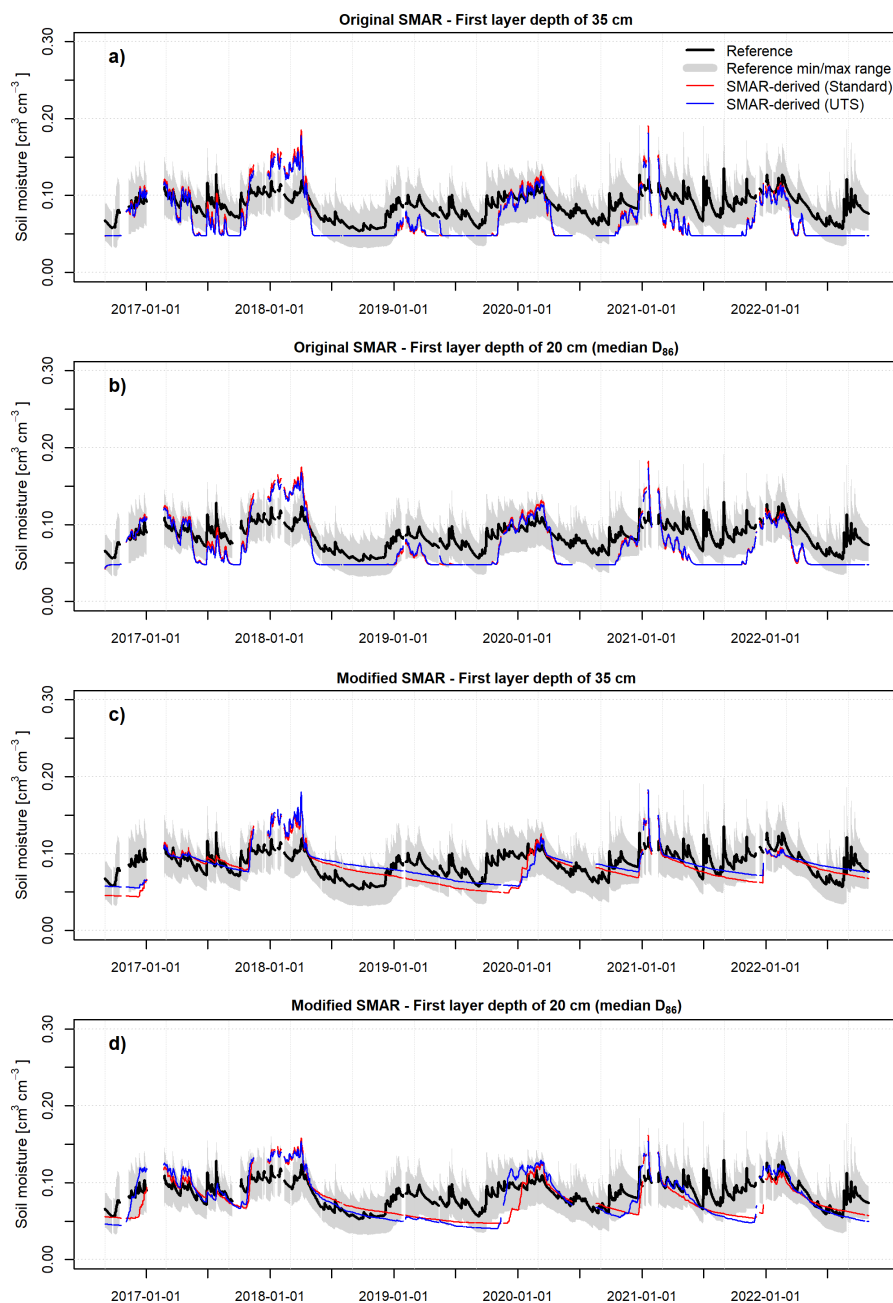


Figure 7. Daily depth-extrapolated soil moisture time series for a depth of 130 cm using the standard SMAR model with a top layer depth of 35 cm (a), and 20 cm (b) as well as the depth-extrapolated soil moisture time series based on the modified SMAR model presented in this study (top layer depth of 35 cm (c) and 20 cm (d)) based on the CRNS-derived surface soil moisture time series from the standard transfer function and the UTS. The soil physical parameters n_1 , n_2 , sc_1 , sc_2 , sw_2 and R_1 were optimized by reducing the RMSE against reference soil moisture values in the year 2017. For the original SMAR model, the water loss term V_2 was calibrated instead of R_1 .



4 Conclusions

In the present study we investigated the feasibility of depth-extrapolating surface soil moisture time series derived from CRNS to deeper soil layers without additional in-situ soil moisture information for calibration. We furthermore evaluated the Universal Transport Solution (UTS) for the estimation of field scale soil moisture from CRNS neutron counts.

515 Being among the first who evaluate the UTS as a new transfer function to estimate field-scale surface soil moisture information from CRNS, we confirm its improved performance compared to the standard approach. The UTS accounts for the interdependence of soil moisture and air humidity on the observed neutron intensity, being most important for dry soil conditions. Although applied at a forested site with rather dry soils but with large amounts of above-ground hydrogen stored in the local biomass and influencing the neutron signal, CRNS-derived soil moisture estimates can be improved compared to using
520 established transfer functions. Thus, our results suggest that the UTS should be used for an improved estimation of surface soil moisture in future CRNS research and applications.

We modified SMAR for estimating soil moisture times series in a second, deeper layer in a way that it can be applied without calibration against in-situ sensors and with soil physical properties and the cumulative root fraction as a vegetation parameter only. Our analyses show that for a benchmark RMSE of $\leq 0.06 \text{ cm}^3 \text{ cm}^{-3}$, the uncalibrated modified SMAR can compete with
525 the original SMAR model down to a maximum depth of the second soil layer of 450 cm when the same soil physical properties are assigned and only the water loss term is calibrated. A certain robustness of the uncalibrated, modified SMAR in terms of the RMSE was shown by sensitivity runs of the model. However, major temporal dynamics of the reference in-situ soil moisture in the second soil layer are neither captured by original nor by the modified SMAR. This is likely linked to the location of the study site in a mixed forest site with sandy soils, accompanied with preferential flow and root water uptake processes that are
530 difficult to simulate, especially with rather simple modeling approaches. Only the use of SMAR with calibrated effective albedo non-physical parameters partly accommodates to the specific soil hydraulic processes at the study site, showing an improved simulation of soil moisture dynamics in a second soil layer. Under these circumstances, deeper soil moisture time series may be more satisfactorily simulated even with simple modeling approaches such as SMAR.

Although our study suggests that improved surface soil moisture estimates from CRNS do not translate to distinctly improved
535 soil moisture estimates in greater depths, a more accurate estimation of the representative measurement depth of CRNS leads to better results of the SMAR model. This indicates that an accurate estimation of the representative measurement depth of CRNS is especially important when using CRNS data as input for hydrological models.

Given the overall performance of the SMAR model at our single study site, further research and testing of the presented modified version of the SMAR model with and without calibration at sites with varying climatic conditions, vegetation cover
540 and soil properties is necessary and encouraged for future studies. Despite the overall unsatisfactory performance of the SMAR model with respect to accurately capturing soil moisture dynamics at our study site, meeting the defined RMSE benchmark, the simple modification of the SMAR algorithm may serve as a valuable first estimate of soil moisture from a second, deeper soil layer, when in-situ reference soil moisture information for calibration are not available and the soil physical parameters can be reasonably well estimated.



545 In CRNS research, this modified SMAR approach opens up potential for roving CRNS, i.e., by mounting CRNS instruments
 on cars (e.g., Schrön et al., 2018a) or trains (e.g., Schrön et al., 2021; Altdorff et al., 2023) moving beyond the field-scale of
 stationary CRNS applications, thereby providing valuable information for landscape water balancing or hydrological catchment
 models on larger scales. Moreover, the modified SMAR approach introduced in this study is not limited to CRNS applications.
 It may also be used in estimating root-zone soil moisture in greater depths from satellite derived surface soil moisture in which
 550 the original SMAR already proved useful (e.g., Baldwin et al., 2017, 2019; Gheybi et al., 2019).

Data availability. All data sets are available from the authors upon request.

Appendix A

Table A1. Minimum and maximum RMSE values between the depth-extrapolated soil moisture time from CRNS using the modified SMAR model of the 50 ensemble runs and the reference soil moisture time series in the second layer calculated from the available in-situ point-scale soil moisture sensors for the simulations with hourly and daily resolution.

| Transfer function | Layer 1 depth [cm] | Layer 2 depth [cm] | Hourly resolution | | Daily resolution | |
|-------------------|--------------------|--------------------|---|---|---|---|
| | | | RMSE _{min} [cm ³ cm ⁻³] | RMSE _{max} [cm ³ cm ⁻³] | RMSE _{min} [cm ³ cm ⁻³] | RMSE _{max} [cm ³ cm ⁻³] |
| Revised standard | 35 | 70 | 0.040 | 0.073 | 0.037 | 0.072 |
| | | 130 | 0.029 | 0.049 | 0.025 | 0.049 |
| | | 200 | 0.027 | 0.044 | 0.023 | 0.045 |
| | | 300 | 0.026 | 0.047 | 0.025 | 0.047 |
| | | 450 | 0.034 | 0.057 | 0.032 | 0.058 |
| | 20 | 70 | 0.032 | 0.052 | 0.027 | 0.049 |
| | | 130 | 0.027 | 0.042 | 0.024 | 0.038 |
| | | 200 | 0.026 | 0.04 | 0.023 | 0.034 |
| | | 300 | 0.025 | 0.043 | 0.02 | 0.035 |
| | | 450 | 0.031 | 0.052 | 0.023 | 0.043 |
| UTS MCNP drf | 35 | 70 | 0.037 | 0.070 | 0.035 | 0.070 |
| | | 130 | 0.028 | 0.048 | 0.024 | 0.049 |
| | | 200 | 0.027 | 0.043 | 0.022 | 0.045 |
| | | 300 | 0.024 | 0.047 | 0.024 | 0.047 |
| | | 450 | 0.032 | 0.057 | 0.032 | 0.059 |
| | 20 | 70 | 0.031 | 0.051 | 0.026 | 0.049 |
| | | 130 | 0.027 | 0.041 | 0.023 | 0.037 |
| | | 200 | 0.026 | 0.04 | 0.022 | 0.033 |
| | | 300 | 0.024 | 0.043 | 0.019 | 0.035 |
| | | 450 | 0.03 | 0.051 | 0.023 | 0.044 |

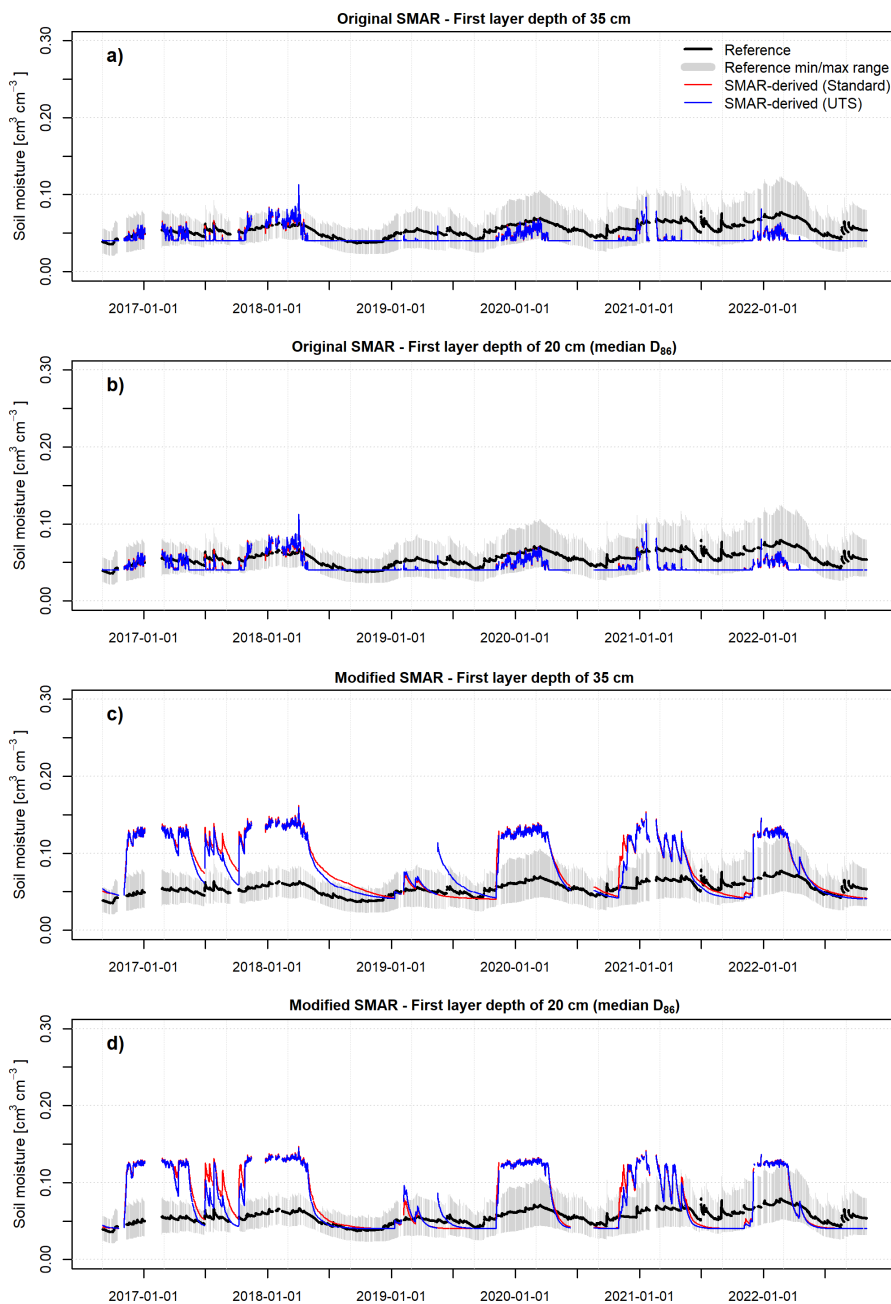


Figure A1. Hourly depth-extrapolated soil moisture time series for a depth of 450 cm using the calibrated standard SMAR model (calibrated water loss V_2) with a top layer depth of 35 cm (a), and 20 cm (b) as well as the depth-extrapolated soil moisture time series based on the uncalibrated modified SMAR (estimated water loss) model presented in this study (top layer depth of 35 cm (c) and 20 cm (d)) based on the CRNS-derived surface soil moisture time series from the standard transfer function and the UTS.

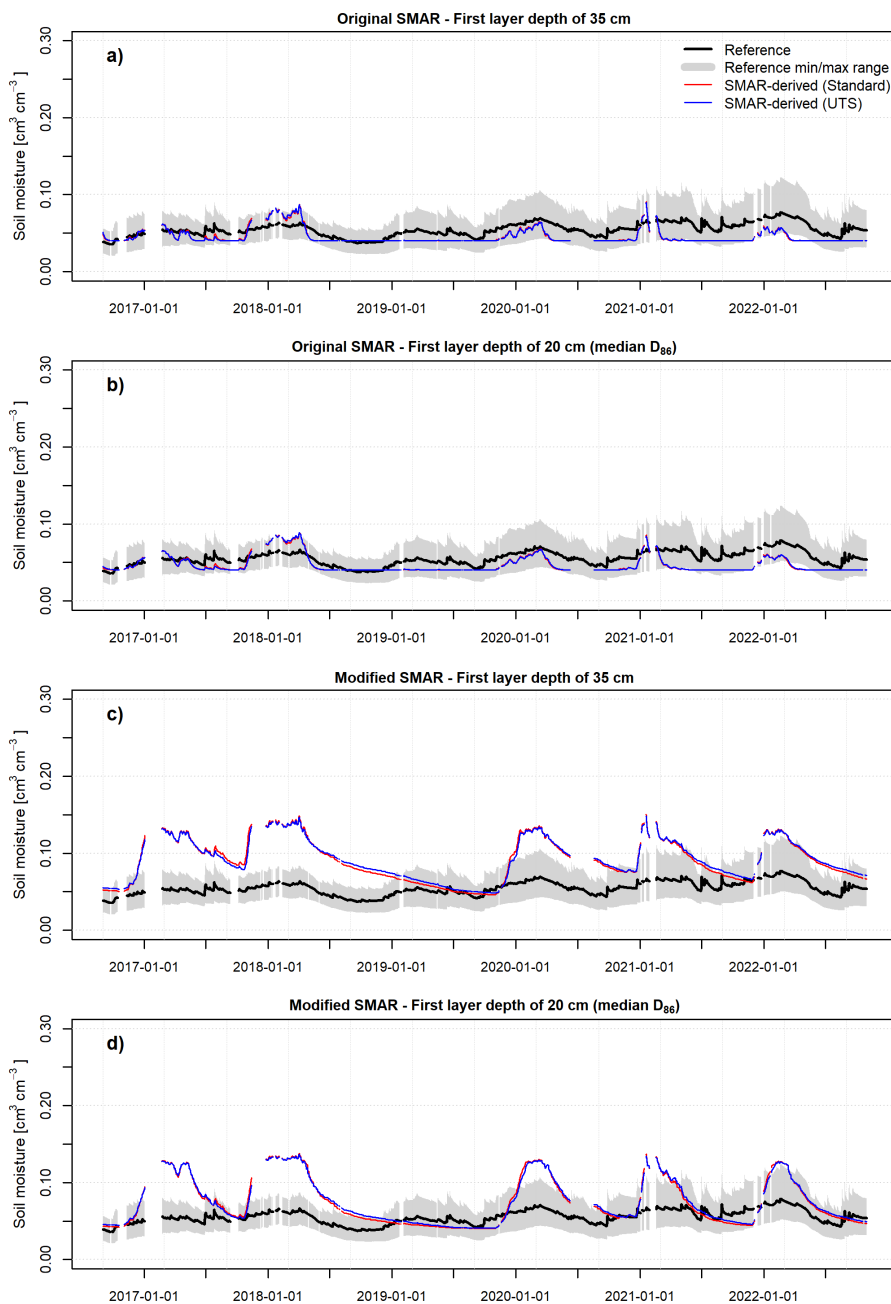


Figure A2. Daily depth-extrapolated soil moisture time series for a depth of 450 cm using the calibrated standard SMAR model (calibrated water loss V_2) with a top layer depth of 35 cm (a), and 20 cm (b) as well as the depth-extrapolated soil moisture time series based on the uncalibrated modified SMAR (estimated water loss) model presented in this study (top layer depth of 35 cm (c) and 20 cm (d)) based on the CRNS-derived surface soil moisture time series from the standard transfer function and the UTS.

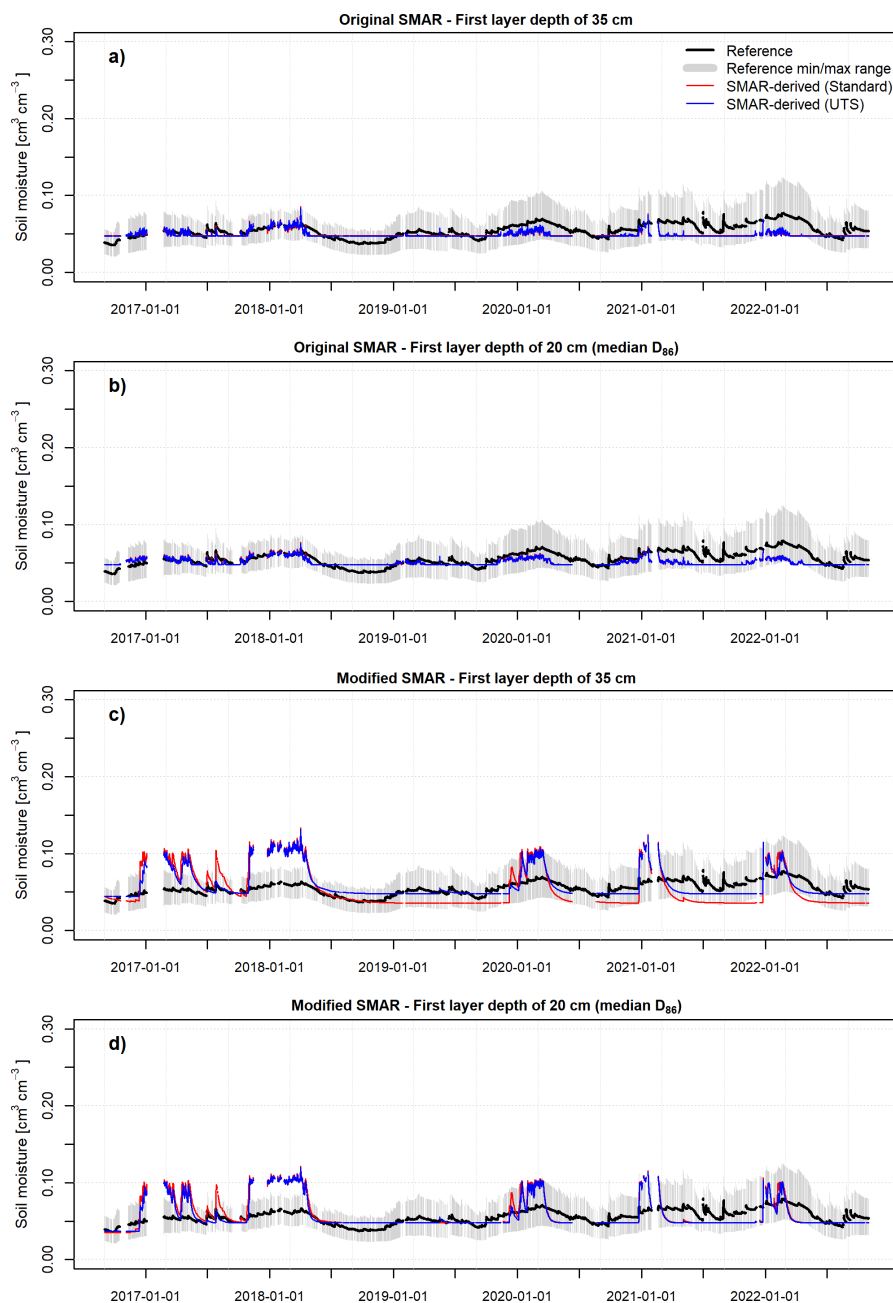


Figure A3. Hourly depth-extrapolated soil moisture time series for a depth of 450 cm using the standard SMAR model with a top layer depth of 35 cm (a), and 20 cm (b) as well as the depth-extrapolated soil moisture time series based on the modified SMAR model presented in this study (top layer depth of 35 cm (c) and 20 cm (d)) based on the CRNS-derived surface soil moisture time series from the standard transfer function and the UTS. The soil physical parameters n_1 , n_2 , sc_1 , sc_2 , sw_2 and R_l were optimized by reducing the RMSE against reference soil moisture values in the year 2017. For the original SMAR model, the water loss term V_2 was calibrated instead of R_l .

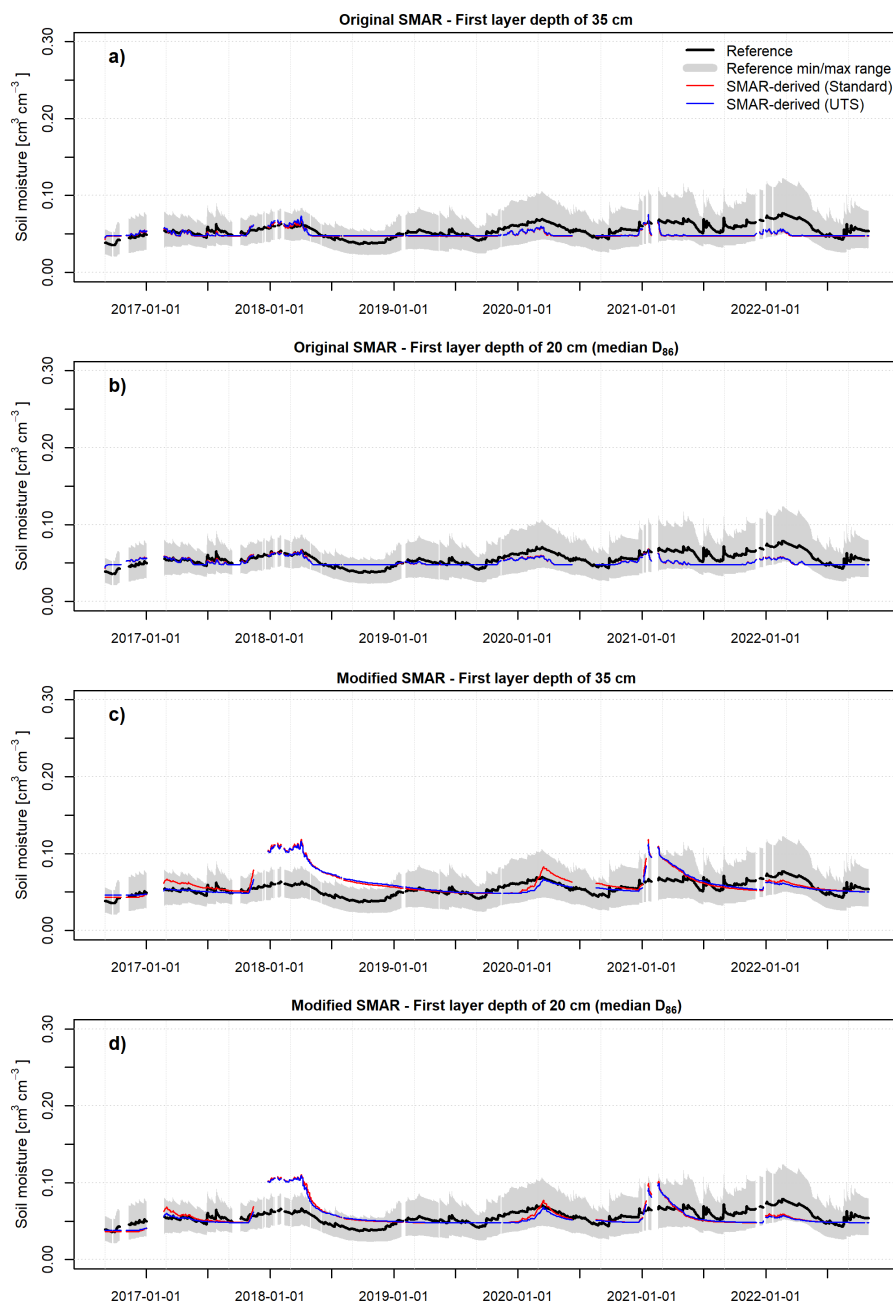


Figure A4. Daily depth-extrapolated soil moisture time series for a depth of 450 cm using the standard SMAR model with a top layer depth of 35 cm (a), and 20 cm (b) as well as the depth-extrapolated soil moisture time series based on the modified SMAR model presented in this study (top layer depth of 35 cm (c) and 20 cm (d)) based on the CRNS-derived surface soil moisture time series from the standard transfer function and the UTS. The soil physical parameters n_1 , n_2 , sc_1 , sc_2 , sw_2 and R_f were optimized by reducing the RMSE against reference soil moisture values in the year 2017. For the original SMAR model, the water loss term V_2 was calibrated instead of R_f .



Table A2. Statistical goodness-of-fit between the depth-extrapolated *hourly* surface soil moisture time series from CRNS and the average soil moisture time series in the second layer calculated from the available in-situ point-scale soil moisture sensors with the fully calibrated SMAR and effective parameters in a non-physically based value range. The calibrated model parameters and goodness-of-fit indicators for the original and modified SMAR model are shown.

| Layer 2 depth [cm] | Layer 1 depth [cm] | Transfer function | SMAR | n_1 [-] | n_2 [-] | sc_1 [$\text{cm}^3 \text{cm}^{-3}$] | sc_2 [$\text{cm}^3 \text{cm}^{-3}$] | sw_2 [$\text{cm}^3 \text{cm}^{-3}$] | V_2 [mm h^{-1}] | R_1 [-] | RMSE [$\text{cm}^3 \text{cm}^{-3}$] | Pearson correlation | KGE [-] | |
|--------------------|--------------------|-------------------|------------------|-----------|-----------|---|---|---|------------------------------|-----------|---------------------------------------|---------------------|---------|--------|
| 70 | 35 | Revised standard | Modified | 0.44 | 0.33 | -0.25 | -0.96 | -0.45 | - | 0.77 | 0.057 | 0.847 | -2.014 | |
| | | | Original | 0.55 | 0.35 | -0.03 | -0.25 | -0.10 | 393 | - | 0.054 | 0.846 | -1.948 | |
| | | UTS MCNP drf | Modified | 0.44 | 0.37 | 0.04 | -0.88 | -0.02 | - | 0.65 | 0.045 | 0.836 | -1.488 | |
| | | | Original | 0.55 | 0.35 | -0.03 | -0.25 | -0.1 | 393 | - | 0.047 | 0.836 | -1.552 | |
| | | 20 | Revised standard | Modified | 0.73 | 0.36 | -0.72 | -0.88 | -0.38 | - | 0.51 | 0.015 | 0.849 | 0.458 |
| | | | | Original | 0.59 | 0.46 | 0.02 | -0.3 | 0.03 | 452 | - | 0.016 | 0.849 | 0.423 |
| | UTS MCNP drf | Modified | 0.73 | 0.36 | -0.72 | -0.88 | -0.38 | - | 0.51 | 0.013 | 0.841 | 0.602 | | |
| | | Original | 0.64 | 0.31 | 0 | -0.07 | 0.03 | 353 | - | 0.012 | 0.841 | 0.627 | | |
| | 130 | 35 | Revised standard | Modified | 0.42 | 0.38 | -0.96 | -0.87 | -0.54 | - | 0.73 | 0.016 | 0.839 | 0.447 |
| | | | | Original | 0.54 | 0.34 | 0.01 | -0.22 | 0.01 | 358 | - | 0.025 | 0.838 | 0.007 |
| | | | UTS MCNP drf | Modified | 0.42 | 0.38 | -0.96 | -0.87 | -0.54 | - | 0.73 | 0.014 | 0.829 | 0.558 |
| | | | | Original | 0.54 | 0.34 | 0.01 | -0.22 | 0.01 | 358 | - | 0.022 | 0.829 | 0.199 |
| 20 | | | Revised standard | Modified | 0.66 | 0.38 | -0.53 | -0.09 | -0.75 | - | 0.45 | 0.008 | 0.855 | 0.790 |
| | | | | Original | 0.64 | 0.37 | -0.23 | -0.48 | -0.01 | 497 | - | 0.009 | 0.855 | 0.839 |
| UTS MCNP drf | | Modified | 0.66 | 0.38 | -0.53 | -0.09 | -0.75 | - | 0.45 | 0.009 | 0.847 | 0.717 | | |
| | | Original | 0.64 | 0.37 | -0.23 | -0.48 | -0.01 | 497 | - | 0.009 | 0.846 | 0.781 | | |
| 200 | | 35 | Revised standard | Modified | 0.45 | 0.31 | -0.79 | -0.58 | -0.19 | - | 0.68 | 0.011 | 0.794 | 0.782 |
| | | | | Original | 0.53 | 0.31 | 0 | -0.07 | 0.03 | 353 | - | 0.015 | 0.794 | 0.366 |
| | | | UTS MCNP drf | Modified | 0.45 | 0.31 | -0.79 | -0.58 | -0.19 | - | 0.68 | 0.010 | 0.788 | 0.750 |
| | | | | Original | 0.53 | 0.31 | 0 | -0.07 | 0.03 | 353 | - | 0.013 | 0.512 | 0.787 |
| | 20 | | Revised standard | Modified | 0.71 | 0.38 | -0.68 | -0.33 | -0.07 | - | 0.51 | 0.009 | 0.811 | 0.563 |
| | | | | Original | 0.54 | 0.32 | -0.90 | -0.75 | -0.22 | 479 | - | 0.014 | 0.811 | 0.739 |
| | UTS MCNP drf | Modified | 0.71 | 0.38 | -0.68 | -0.33 | -0.07 | - | 0.51 | 0.009 | 0.805 | 0.504 | | |
| | | Original | 0.75 | 0.37 | -0.96 | -0.53 | -0.27 | 498 | - | 0.012 | 0.805 | 0.749 | | |
| | 300 | 35 | Revised standard | Modified | 0.49 | 0.36 | -0.93 | -0.60 | -0.12 | - | 0.71 | 0.009 | 0.733 | 0.658 |
| | | | | Original | 0.54 | 0.34 | 0.01 | -0.22 | 0.01 | 358 | - | 0.022 | 0.734 | -0.042 |
| | | | UTS MCNP drf | Modified | 0.49 | 0.36 | -0.93 | -0.60 | -0.12 | - | 0.71 | 0.009 | 0.728 | 0.602 |
| | | | | Original | 0.54 | 0.34 | 0.01 | -0.22 | 0.01 | 358 | - | 0.019 | 0.729 | 0.147 |
| 20 | | | Revised standard | Modified | 0.61 | 0.33 | -0.79 | -0.02 | -0.85 | - | 0.49 | 0.009 | 0.751 | 0.393 |
| | | | | Original | 0.70 | 0.35 | -0.09 | -0.73 | 0.02 | 374 | - | 0.009 | 0.751 | 0.739 |
| UTS MCNP drf | | Modified | 0.61 | 0.33 | -0.79 | -0.02 | -0.85 | - | 0.49 | 0.009 | 0.746 | 0.350 | | |
| | | Original | 0.70 | 0.35 | -0.09 | -0.73 | 0.02 | 374 | - | 0.009 | 0.747 | 0.738 | | |
| 450 | | 35 | Revised standard | Modified | 0.55 | 0.32 | -0.24 | -0.44 | 0.01 | - | 0.65 | 0.010 | 0.593 | 0.448 |
| | | | | Original | 0.54 | 0.37 | 0.06 | -0.42 | 0.02 | 448 | - | 0.019 | 0.577 | 0.045 |
| | | | UTS MCNP drf | Modified | 0.55 | 0.32 | -0.24 | -0.44 | 0.01 | - | 0.65 | 0.010 | 0.592 | 0.404 |
| | | | | Original | 0.54 | 0.37 | 0.06 | -0.42 | 0.02 | 448 | - | 0.018 | 0.586 | 0.139 |
| | 20 | | Revised standard | Modified | 0.54 | 0.44 | -0.27 | -0.70 | 0.03 | - | 0.46 | 0.009 | 0.619 | 0.232 |
| | | | | Original | 0.64 | 0.37 | -0.23 | -0.48 | -0.01 | 497 | - | 0.009 | 0.618 | 0.609 |
| | UTS MCNP drf | Modified | 0.54 | 0.44 | -0.27 | -0.70 | 0.03 | - | 0.46 | 0.009 | 0.618 | 0.202 | | |
| | | Original | 0.64 | 0.37 | -0.23 | -0.48 | -0.01 | 497 | - | 0.008 | 0.619 | 0.616 | | |



Table A3. Statistical goodness-of-fit between the depth-extrapolated *daily* surface soil moisture time from CRNS and the average soil moisture time series in the second layer calculated from the available in-situ point-scale soil moisture sensors with the fully calibrated SMAR and effective parameters in a non-physically based value range. The calibrated model parameters and goodness-of-fit indicators for the original and modified SMAR model are shown.

| Layer 2 depth [cm] | Layer 1 depth [cm] | Transfer function | SMAR | n_1 [-] | n_2 [-] | sc_1 [$\text{cm}^3 \text{cm}^{-3}$] | sc_2 [$\text{cm}^3 \text{cm}^{-3}$] | sw_2 [$\text{cm}^3 \text{cm}^{-3}$] | V_2 [mm h^{-1}] | R_1 [-] | RMSE [$\text{cm}^3 \text{cm}^{-3}$] | Pearson correlation | KGE [-] | |
|--------------------|--------------------|-------------------|------------------|-----------|-----------|---|---|---|------------------------------|-----------|---------------------------------------|---------------------|---------|-------|
| 70 | 35 | Revised standard | Modified | 0.42 | 0.43 | 0.11 | -0.82 | 0.04 | - | 0.61 | 0.033 | 0.764 | -0.555 | |
| | | | Original | 0.45 | 0.37 | 0.01 | 0.34 | -0.05 | 488 | - | 0.052 | 0.854 | -1.806 | |
| | | UTS MCNP drf | Modified | 0.48 | 0.31 | 0.09 | -0.76 | 0.04 | - | 0.64 | 0.032 | 0.804 | -0.743 | |
| | | | Original | 0.45 | 0.37 | 0.01 | -0.34 | -0.05 | 488 | - | 0.046 | 0.844 | -1.42 | |
| | | 20 | Revised standard | Modified | 0.74 | 0.33 | 0 | -0.77 | 0.03 | - | 0.54 | 0.013 | 0.856 | 0.521 |
| | | | | Original | 0.74 | 0.34 | -0.06 | -0.69 | 0 | 452 | - | 0.015 | 0.856 | 0.482 |
| | UTS MCNP drf | Modified | 0.74 | 0.33 | 0 | -0.77 | 0.03 | - | 0.54 | 0.012 | 0.848 | 0.658 | | |
| | | Original | 0.68 | 0.33 | -0.02 | -0.03 | 0.02 | 391 | - | 0.012 | 0.848 | 0.619 | | |
| | 130 | 35 | Revised standard | Modified | 0.61 | 0.33 | 0 | -0.77 | 0.03 | - | 0.78 | 0.016 | 0.843 | 0.536 |
| | | | | Original | 0.48 | 0.32 | 0.04 | -0.86 | 0.04 | 477 | - | 0.013 | 0.840 | 0.378 |
| | | | UTS MCNP drf | Modified | 0.60 | 0.31 | -0.43 | -0.80 | -0.16 | - | 0.63 | 0.013 | 0.835 | 0.641 |
| | | | | Original | 0.48 | 0.32 | 0.04 | -0.86 | 0.04 | 477 | - | 0.016 | 0.835 | 0.502 |
| 20 | | | Revised standard | Modified | 0.55 | 0.39 | -0.68 | -0.14 | -0.70 | - | 0.46 | 0.008 | 0.862 | 0.798 |
| | | | | Original | 0.64 | 0.37 | -0.23 | -0.48 | -0.01 | 497 | - | 0.009 | 0.846 | 0.846 |
| UTS MCNP drf | | Modified | 0.73 | 0.43 | -0.29 | -0.03 | -0.69 | - | 0.46 | 0.008 | 0.854 | 0.769 | | |
| | | Original | 0.65 | 0.38 | -0.04 | -0.64 | 0.04 | 423 | - | 0.008 | 0.854 | 0.808 | | |
| 200 | | 35 | Revised standard | Modified | 0.47 | 0.31 | -0.33 | -0.71 | -0.03 | - | 0.73 | 0.01 | 0.798 | 0.775 |
| | | | | Original | 0.61 | 0.34 | -0.06 | -0.69 | 0 | 452 | - | 0.018 | 0.804 | 0.383 |
| | | | UTS MCNP drf | Modified | 0.47 | 0.31 | -0.33 | -0.71 | -0.03 | - | 0.73 | 0.010 | 0.792 | 0.727 |
| | | | | Original | 0.61 | 0.34 | -0.06 | -0.69 | 0 | 452 | - | 0.016 | 0.797 | 0.527 |
| | 20 | | Revised standard | Modified | 0.72 | 0.42 | -0.93 | -0.19 | -0.29 | - | 0.43 | 0.009 | 0.820 | 0.617 |
| | | | | Original | 0.73 | 0.33 | -0.19 | -0.13 | 0.01 | 421 | - | 0.009 | 0.822 | 0.769 |
| | UTS MCNP drf | Modified | 0.59 | 0.45 | -0.39 | -0.03 | -0.39 | - | 0.39 | 0.009 | 0.814 | 0.608 | | |
| | | Original | 0.61 | 0.31 | -0.08 | -0.23 | 0.04 | 409 | - | 0.009 | 0.814 | 0.644 | | |
| | 300 | 35 | Revised standard | Modified | 0.55 | 0.40 | -0.54 | -1 | -0.03 | - | 0.56 | 0.008 | 0.741 | 0.626 |
| | | | | Original | 0.48 | 0.32 | 0.04 | -0.86 | 0.04 | 477 | - | 0.012 | 0.747 | 0.502 |
| | | | UTS MCNP drf | Modified | 0.55 | 0.40 | -0.54 | -1 | -0.03 | - | 0.56 | 0.008 | 0.736 | 0.567 |
| | | | | Original | 0.48 | 0.32 | 0.04 | -0.86 | 0.04 | 477 | - | 0.011 | 0.744 | 0.597 |
| 20 | | | Revised standard | Modified | 0.57 | 0.46 | -0.28 | 0.02 | -0.57 | - | 0.40 | 0.008 | 0.764 | 0.504 |
| | | | | Original | 0.67 | 0.33 | -0.39 | -0.49 | -0.04 | 442 | - | 0.009 | 0.771 | 0.760 |
| UTS MCNP drf | | Modified | 0.66 | 0.39 | 0.06 | 0.06 | -0.39 | - | 0.50 | 0.024 | 0.666 | -0.429 | | |
| | | Original | 0.67 | 0.33 | -0.39 | -0.49 | -0.04 | 442 | - | 0.008 | 0.766 | 0.747 | | |
| 450 | | 35 | Revised standard | Modified | 0.55 | 0.34 | -0.20 | -0.91 | 0.02 | - | 0.74 | 0.009 | 0.604 | 0.405 |
| | | | | Original | 0.42 | 0.35 | 0 | -0.17 | 0.01 | 487 | - | 0.016 | 0.619 | 0.067 |
| | | | UTS MCNP drf | Modified | 0.44 | 0.37 | -0.82 | -0.83 | -0.04 | - | 0.54 | 0.008 | 0.604 | 0.387 |
| | | | | Original | 0.42 | 0.35 | 0 | -0.17 | 0.01 | 487 | - | 0.015 | 0.617 | 0.23 |
| | 20 | | Revised standard | Modified | 0.71 | 0.39 | -1 | -0.04 | -0.47 | - | 0.41 | 0.008 | 0.637 | 0.339 |
| | | | | Original | 0.64 | 0.31 | -0.33 | -0.13 | -0.03 | 456 | - | 0.011 | 0.649 | 0.618 |
| | UTS MCNP drf | Modified | 0.54 | 0.34 | -0.65 | 0 | -0.66 | - | 0.41 | 0.008 | 0.633 | 0.260 | | |
| | | Original | 0.64 | 0.31 | -0.33 | -0.13 | -0.03 | 456 | - | 0.010 | 0.647 | 0.627 | | |

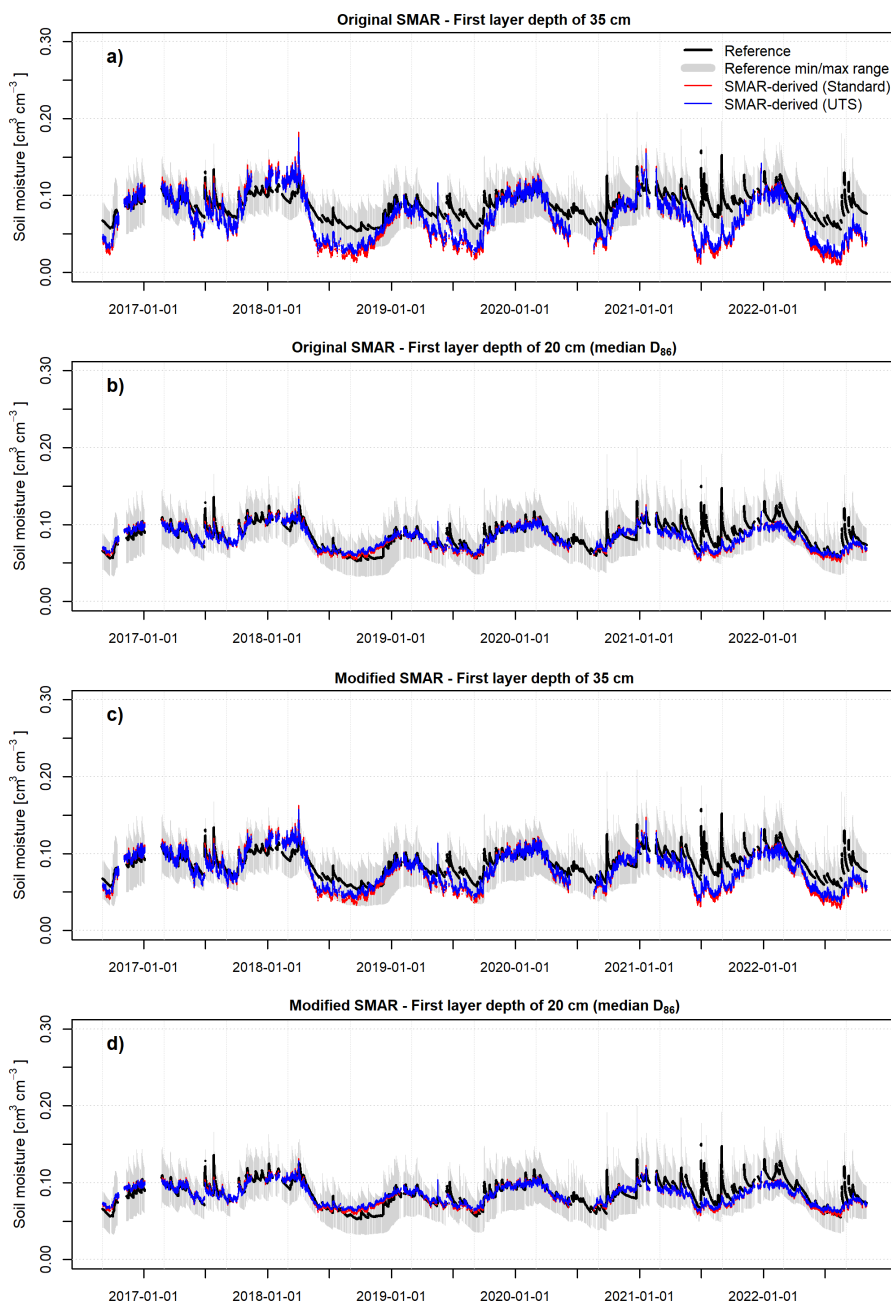


Figure A5. Hourly depth-extrapolated soil moisture time series for a depth of 130 cm using the standard SMAR model with a top layer depth of 35 cm (a), and 20 cm (b) as well as the depth-extrapolated soil moisture time series based on the modified SMAR model presented in this study (top layer depth of 35 cm (c) and 20 cm (d)) based on the CRNS-derived surface soil moisture time series from the standard transfer function and the UTS. The soil physical parameters n_1 , n_2 , sc_1 , sc_2 , sw_2 and R_1 were optimized by reducing the RMSE against reference soil moisture values in the year 2017. Here, the parameters sc_1 , sc_2 and sw_2 were calibrated as effective parameters in a non-physically based value range. For the original SMAR model, the water loss term V_2 was calibrated instead of R_1 .

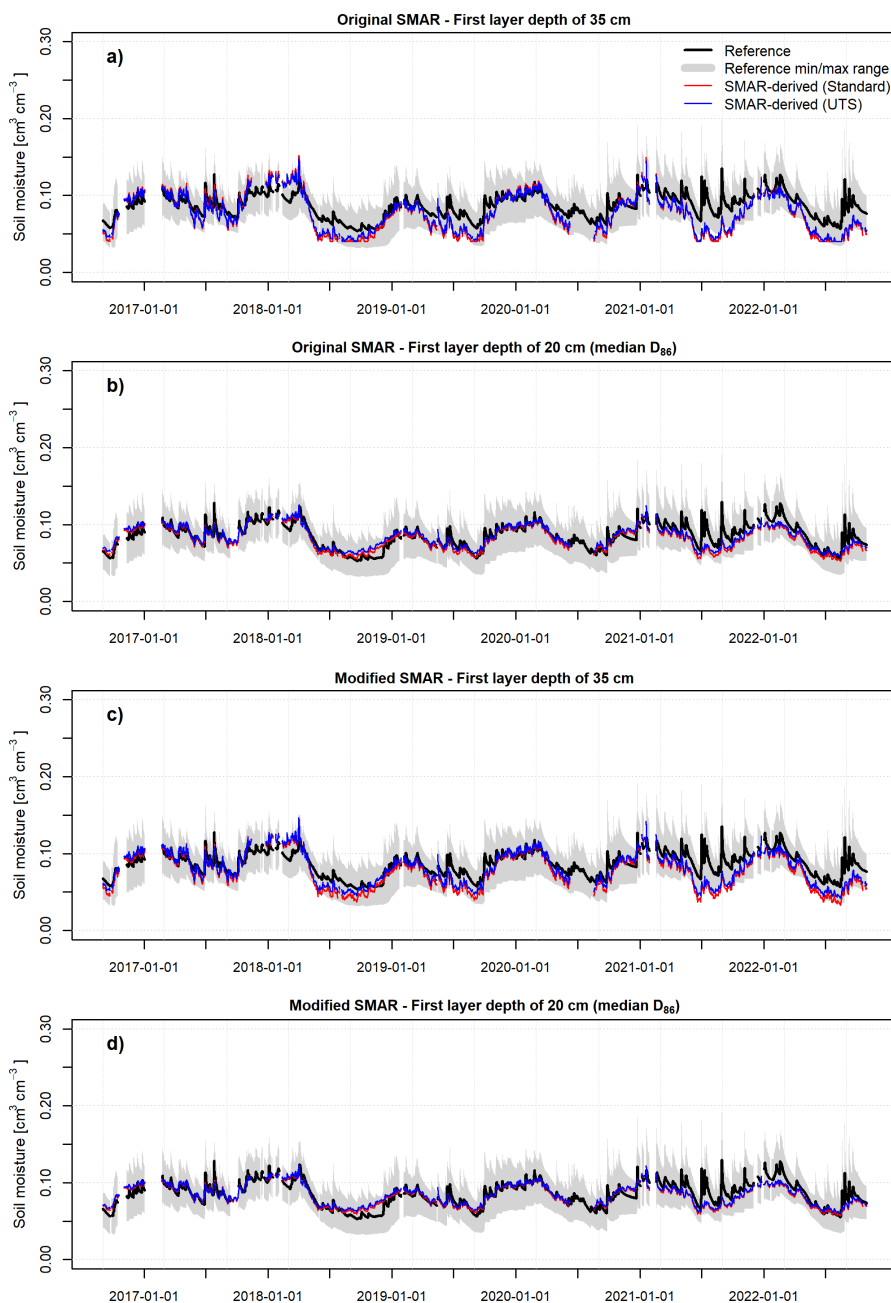


Figure A6. Daily depth-extrapolated soil moisture time series for a depth of 130 cm using the standard SMAR model with a top layer depth of 35 cm (a), and 20 cm (b) as well as the depth-extrapolated soil moisture time series based on the modified SMAR model presented in this study (top layer depth of 35 cm (c) and 20 cm (d)) based on the CRNS-derived surface soil moisture time series from the standard transfer function and the UTS. The soil physical parameters n_1 , n_2 , sc_1 , sc_2 , sw_2 and R_1 were optimized by reducing the RMSE against reference soil moisture values in the year 2017. Here, the parameters sc_1 , sc_2 and sw_2 were calibrated as effective parameters in a non-physically based value range. For the original SMAR model, the water loss term V_2 was calibrated instead of R_1 .

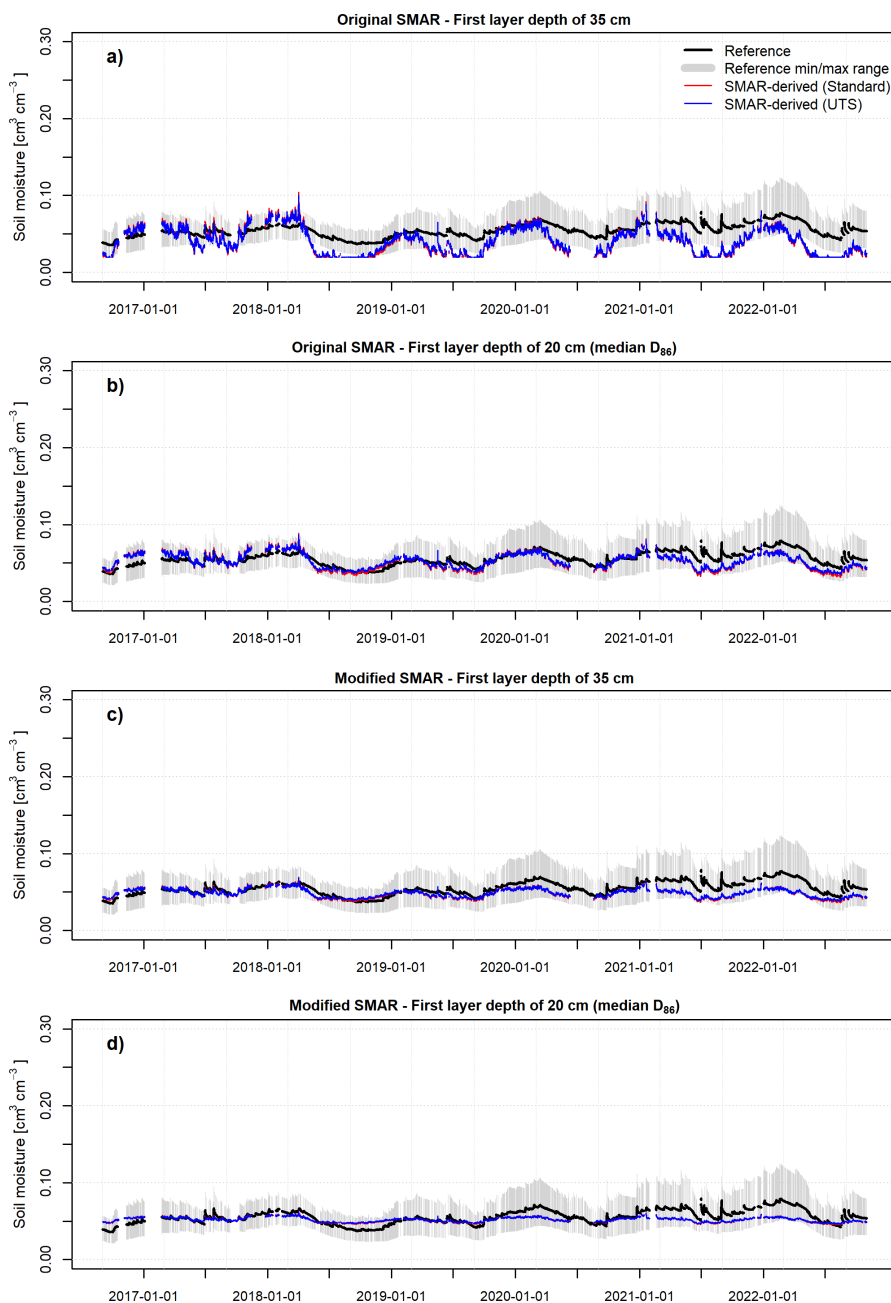


Figure A7. Hourly depth-extrapolated soil moisture time series for a depth of 450 cm using the standard SMAR model with a top layer depth of 35 cm (a), and 20 cm (b) as well as the depth-extrapolated soil moisture time series based on the modified SMAR model presented in this study (top layer depth of 35 cm (c) and 20 cm (d)) based on the CRNS-derived surface soil moisture time series from the standard transfer function and the UTS. The soil physical parameters n_1 , n_2 , sc_1 , sc_2 , sw_2 and R_1 were optimized by reducing the RMSE against reference soil moisture values in the year 2017. Here, the parameters sc_1 , sc_2 and sw_2 were calibrated as effective parameters in a non-physically based value range. For the original SMAR model, the water loss term V_2 was calibrated instead of R_1 .

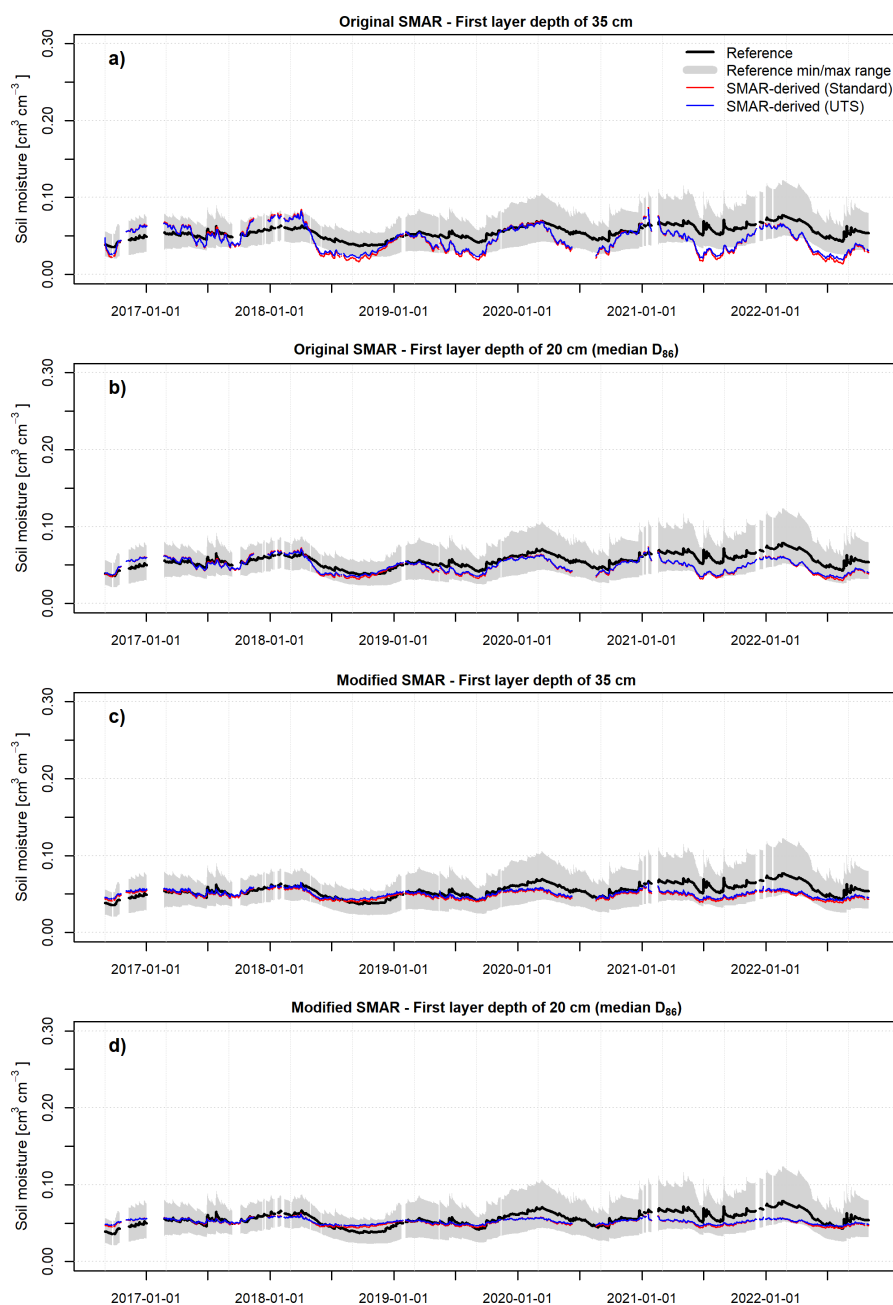


Figure A8. Daily depth-extrapolated soil moisture time series for a depth of 450 cm using the standard SMAR model with a top layer depth of 35 cm (a), and 20 cm (b) as well as the depth-extrapolated soil moisture time series based on the modified SMAR model presented in this study (top layer depth of 35 cm (c) and 20 cm (d)) based on the CRNS-derived surface soil moisture time series from the standard transfer function and the UTS. The soil physical parameters n_1 , n_2 , sc_1 , sc_2 , sw_2 and R_f were optimized by reducing the RMSE against reference soil moisture values in the year 2017. Here, the parameters sc_1 , sc_2 and sw_2 were calibrated as effective parameters in a non-physically based value range. For the original SMAR model, the water loss term V_2 was calibrated instead of R_f .



Author contributions. DR further developed the original ideas of TB and AG for this study, performed the data analysis and wrote the manuscript. TB and AG designed the soil moisture monitoring network and contributed to the writing of the manuscript.

555 *Competing interests.* The authors declare no competing interests.

Acknowledgements. This study was conducted as part of the research unit Cosmic Sense funded by the German Research Foundation (Deutsche Forschungsgemeinschaft, DFG-FOR2694, project no. 357874777). We gratefully acknowledge the technical support of Markus Morgner, Jörg Wummel and Stephan Schröder who maintain the observation sites in TERENO-NE funded by the Helmholtz Association. In addition, we would like to thank Paul Voit for his assistance in data acquisition, field and laboratory work. Further, we would like to thank the

560 Müritz National Park for the continuing support and collaboration. Lastly, we acknowledge the NMDB database (www.nmdb.eu) founded under the European Union's FP7 programme (contract no. 213007), and the PIs of individual neutron monitors for providing data.



References

- Alaoui, A., Caduff, U., Gerke, H., and Weingartner, R.: Preferential Flow Effects on Infiltration and Runoff in Grassland and Forest Soils, *Vadose Zone Journal*, 10, 367–377, <https://doi.org/10.2136/vzj2010.0076>, 2011.
- 565 Albergel, C., Rüdiger, C., Pellarin, T., Calvet, J.-C., Fritz, N., Froissard, F., Suquia, D., Petitpa, A., Pignatelli, B., and Martin, E.: From near-surface to root-zone soil moisture using an exponential filter: an assessment of the method based on in-situ observations and model simulations, *Hydrology and Earth System Sciences*, 12, 1323–1337, <https://doi.org/10.5194/hess-12-1323-2008>, 2008.
- Altdorff, D., Oswald, S. E., Zacharias, S., Zengerle, C., Dietrich, P., Mollenhauer, H., Attinger, S., and Schrön, M.: Toward Large-Scale Soil Moisture Monitoring Using Rail-Based Cosmic Ray Neutron Sensing, *Water Resources Research*, 59, <https://doi.org/10.1029/2022wr033514>, 2023.
- 570 Andreasen, M., Jensen, K. H., Desilets, D., Franz, T. E., Zreda, M., Bogaen, H. R., and Looms, M. C.: Status and Perspectives on the Cosmic-Ray Neutron Method for Soil Moisture Estimation and Other Environmental Science Applications, *Vadose Zone Journal*, 16, vzj2017.04.0086, <https://doi.org/10.2136/vzj2017.04.0086>, 2017.
- Baatz, R., Bogaen, H. R., Franssen, H.-J. H., Huisman, J. A., Montzka, C., and Vereecken, H.: An empirical vegetation correction for soil water content quantification using cosmic ray probes, *Water Resources Research*, 51, 2030–2046, <https://doi.org/10.1002/2014wr016443>, 2015.
- 575 Babaeian, E., Sadeghi, M., Jones, S. B., Montzka, C., Vereecken, H., and Tuller, M.: Ground, Proximal, and Satellite Remote Sensing of Soil Moisture, *Reviews of Geophysics*, 57, 530–616, <https://doi.org/10.1029/2018rg000618>, 2019.
- Baldwin, D., Manfreda, S., Keller, K., and Smithwick, E.: Predicting root zone soil moisture with soil properties and satellite near-surface moisture data across the conterminous United States, *Journal of Hydrology*, 546, 393–404, <https://doi.org/10.1016/j.jhydrol.2017.01.020>, 2017.
- 580 Baldwin, D., Manfreda, S., Lin, H., and Smithwick, E. A.: Estimating Root Zone Soil Moisture Across the Eastern United States with Passive Microwave Satellite Data and a Simple Hydrologic Model, *Remote Sensing*, 11, 2013, <https://doi.org/10.3390/rs11172013>, 2019.
- Baroni, G. and Oswald, S.: A scaling approach for the assessment of biomass changes and rainfall interception using cosmic-ray neutron sensing, *Journal of Hydrology*, 525, 264–276, <https://doi.org/10.1016/j.jhydrol.2015.03.053>, 2015.
- 585 BKG - German Federal Agency for Cartography and Geodesy: Digital landcover model: ATKIS-Basis-DLM (© GeoBasis-DE/BKG 2018), https://www.bkg.bund.de/SharedDocs/Produktinformationen/BKG/DE/P-2019/191011_ATKISDLM.html, 2018.
- Bogaen, H., Montzka, C., Huisman, J., Graf, A., Schmidt, M., Stockinger, M., von Hebel, C., Hendricks-Franssen, H., van der Kruk, J., Tappe, W., Lücke, A., Baatz, R., Bol, R., Groh, J., Pütz, T., Jakobi, J., Kunkel, R., Sorg, J., and Vereecken, H.: The TERENO-Rur Hydrological Observatory: A Multiscale Multi-Compartment Research Platform for the Advancement of Hydrological Science, *Vadose Zone Journal*, 17, 180055, <https://doi.org/10.2136/vzj2018.03.0055>, 2018.
- 590 Bogaen, H. R., Schrön, M., Jakobi, J., Ney, P., Zacharias, S., Andreasen, M., Baatz, R., Boorman, D., Duygu, M. B., Eguibar-Galán, M. A., Fersch, B., Franke, T., Geris, J., Sanchis, M. G., Kerr, Y., Korf, T., Mengistu, Z., Mialon, A., Nasta, P., Nitychoruk, J., Pinaras, V., Rasche, D., Rosolem, R., Said, H., Schattan, P., Zreda, M., Achleitner, S., Albentosa-Hernández, E., Akyürek, Z., Blume, T., del Campo, A., Canone, D., Dimitrova-Petrova, K., Evans, J. G., Ferraris, S., Frances, F., Gisolo, D., Güntner, A., Herrmann, F., Iwema, J., Jensen, K. H., Kunstmann, H., Lidón, A., Looms, M. C., Oswald, S., Panagopoulos, A., Patil, A., Power, D., Rebmann, C., Romano, N., Scheffele, L., Seneviratne, S., Weltin, G., and Vereecken, H.: COSMOS-Europe: a European network of cosmic-ray neutron soil moisture sensors, *Earth System Science Data*, 14, 1125–1151, <https://doi.org/10.5194/essd-14-1125-2022>, 2022.



- Börner, A.: Neue Beiträge zum Naturraum und zur Landschaftsgeschichte im Teilgebiet Serrahn des Müritz-Nationalparks - Forschung und
600 Monitoring, vol. 4, chap. Geologische Entwicklung des Gebietes um den Großen Fürstenseer See, p. 21–29, Geozon Science Media,
Berlin, <https://doi.org/10.3285/g.00012>, 2015.
- Canadell, J., Jackson, R. B., Ehleringer, J. B., Mooney, H. A., Sala, O. E., and Schulze, E.-D.: Maximum rooting depth of vegetation types
at the global scale, *Oecologia*, 108, 583–595, <https://doi.org/10.1007/bf00329030>, 1996.
- Chandler, K., Stevens, C., Binley, A., and Keith, A.: Influence of tree species and forest land use on soil hydraulic conductivity and implica-
605 tions for surface runoff generation, *Geoderma*, 310, 120–127, <https://doi.org/10.1016/j.geoderma.2017.08.011>, 2018.
- Daly, E. and Porporato, A.: A Review of Soil Moisture Dynamics: From Rainfall Infiltration to Ecosystem Response, *Environmental Engi-
neering Science*, 22, 9–24, <https://doi.org/10.1089/ees.2005.22.9>, 2005.
- Desilets, D., Zreda, M., and Ferré, T. P. A.: Nature's neutron probe: Land surface hydrology at an elusive scale with cosmic rays, *Water
Resources Research*, 46, <https://doi.org/10.1029/2009wr008726>, 2010.
- 610 Dimitrova-Petrova, K., Geris, J., Wilkinson, E. M., Rosolem, R., Verrot, L., Lilly, A., and Soulsby, C.: Opportunities and challenges in
using catchment-scale storage estimates from cosmic ray neutron sensors for rainfall-runoff modelling, *Journal of Hydrology*, p. 124878,
<https://doi.org/10.1016/j.jhydrol.2020.124878>, 2020.
- Dorman, L. I.: *Cosmic Rays in the Earth's Atmosphere and Underground*, Astrophysics and Space Science Library, Springer Netherlands, 1
edn., <https://doi.org/10.1007/978-1-4020-2113-8>, 2004.
- 615 Duygu, M. B. and Akyürek, Z.: Using Cosmic-Ray Neutron Probes in Validating Satellite Soil Moisture Products and Land Surface Models,
Water, 11, 1362, <https://doi.org/10.3390/w11071362>, 2019.
- DWD - German Weather Service: Multi-annual temperature observations 1981-2010, [ftp://opendata.dwd.de/climate_environment/CDC/
observations_germany/climate/multi_annual/mean_81-10/Temperatur_1981-2010_aktStandort.txt](ftp://opendata.dwd.de/climate_environment/CDC/observations_germany/climate/multi_annual/mean_81-10/Temperatur_1981-2010_aktStandort.txt), 2020a.
- DWD - German Weather Service: Multi-annual precipitation observations 1981-2010, [ftp://opendata.dwd.de/climate_environment/CDC/
620 observations_germany/climate/multi_annual/mean_81-10/Niederschlag_1981-2010_aktStandort.txt](ftp://opendata.dwd.de/climate_environment/CDC/observations_germany/climate/multi_annual/mean_81-10/Niederschlag_1981-2010_aktStandort.txt), 2020b.
- Famiglietti, J. S., Ryu, D., Berg, A. A., Rodell, M., and Jackson, T. J.: Field observations of soil moisture variability across scales, *Water
Resources Research*, 44, <https://doi.org/10.1029/2006wr005804>, 2008.
- Fan, Y., Miguez-Macho, G., Jobbágy, E. G., Jackson, R. B., and Otero-Casal, C.: Hydrologic regulation of plant rooting depth, *Proceedings
of the National Academy of Sciences*, 114, 10 572–10 577, <https://doi.org/10.1073/pnas.1712381114>, 2017.
- 625 Faridani, F., Farid, A., Ansari, H., and Manfreda, S.: A modified version of the SMAR model for estimating root-zone soil moisture from
time-series of surface soil moisture, *Water SA*, 43, 492, <https://doi.org/10.4314/wsa.v43i3.14>, 2017.
- Farokhi, M., Faridani, F., Lasaponara, R., Ansari, H., and Faridhosseini, A.: Enhanced Estimation of Root Zone Soil Mois-
ture at 1 km Resolution Using SMAR Model and MODIS-Based Downscaled AMSR2 Soil Moisture Data, *Sensors*, 21, 5211,
<https://doi.org/10.3390/s21155211>, 2021.
- 630 Fersch, B., Jagdhuber, T., Schrön, M., Völsch, I., and Jäger, M.: Synergies for Soil Moisture Retrieval Across Scales From Air-
borne Polarimetric SAR, Cosmic Ray Neutron Roving, and an In Situ Sensor Network, *Water Resources Research*, 54, 9364–9383,
<https://doi.org/10.1029/2018wr023337>, 2018.
- Franz, T. E., Zreda, M., Rosolem, R., and Ferre, T. P. A.: A universal calibration function for determination of soil moisture with cosmic-ray
neutrons, *Hydrology and Earth System Sciences*, 17, 453–460, <https://doi.org/10.5194/hess-17-453-2013>, 2013.
- 635 Franz, T. E., Wahbi, A., Zhang, J., Vreugdenhil, M., Heng, L., Dercon, G., Strauss, P., Brocca, L., and Wagner, W.: Practical Data Products
From Cosmic-Ray Neutron Sensing for Hydrological Applications, *Frontiers in Water*, 2, <https://doi.org/10.3389/frwa.2020.00009>, 2020.



- Gao, X., Zhao, X., Brocca, L., Pan, D., and Wu, P.: Testing of observation operators designed to estimate profile soil moisture from surface measurements, *Hydrological Processes*, 33, 575–584, <https://doi.org/10.1002/hyp.13344>, 2018.
- Gheybi, F., Paridad, P., Faridani, F., Farid, A., Pizarro, A., Fiorentino, M., and Manfreda, S.: Soil Moisture Monitoring in Iran by Implementing Satellite Data into the Root-Zone SMAR Model, *Hydrology*, 6, 44, <https://doi.org/10.3390/hydrology6020044>, 2019.
- 640 Gugerli, R., Salzmann, N., Huss, M., and Desilets, D.: Continuous and autonomous snow water equivalent measurements by a cosmic ray sensor on an alpine glacier, *The Cryosphere*, 13, 3413–3434, <https://doi.org/10.5194/tc-13-3413-2019>, 2019.
- Guo, X., Fang, X., Zhu, Q., Jiang, S., Tian, J., Tian, Q., and Jin, J.: Estimation of Root-Zone Soil Moisture in Semi-Arid Areas Based on Remotely Sensed Data, *Remote Sensing*, 15, 2003, <https://doi.org/10.3390/rs15082003>, 2023.
- 645 Gupta, H. V., Kling, H., Yilmaz, K. K., and Martinez, G. F.: Decomposition of the mean squared error and NSE performance criteria: Implications for improving hydrological modelling, *Journal of Hydrology*, 377, 80–91, <https://doi.org/10.1016/j.jhydrol.2009.08.003>, 2009.
- Heidbüchel, I., Güntner, A., and Blume, T.: Use of cosmic-ray neutron sensors for soil moisture monitoring in forests, *Hydrology and Earth System Sciences*, 20, 1269–1288, <https://doi.org/10.5194/hess-20-1269-2016>, 2016.
- Heinrich, I., Balanzategui, D., Bens, O., Blasch, G., Blume, T., Böttcher, F., Borg, E., Brademann, B., Brauer, A., Conrad, C., Dietze, E., Dräger, N., Fiener, P., Gerke, H. H., Güntner, A., Heine, I., Helle, G., Herbrich, M., Harfenmeister, K., Heußner, K.-U., Hohmann, C., Itzerott, S., Jurasinski, G., Kaiser, K., Kappler, C., Koebsch, F., Liebner, S., Lischeid, G., Merz, B., Missling, K. D., Morgner, M., Pinkerneil, S., Plessen, B., Raab, T., Ruhtz, T., Sachs, T., Sommer, M., Spengler, D., Stender, V., Stüve, P., and Wilken, F.: Interdisciplinary Geo-ecological Research across Time Scales in the Northeast German Lowland Observatory (TERENO-NE), *Vadose Zone Journal*, 17, 180 116, <https://doi.org/10.2136/vzj2018.06.0116>, 2018.
- 650 Holgate, C., Jeu, R. D., van Dijk, A., Liu, Y., Renzullo, L., Vinodkumar, Dharssi, I., Parinussa, R., Schalie, R. V. D., Gevaert, A., Walker, J., McJannet, D., Cleverly, J., Haverd, V., Trudinger, C., and Briggs, P.: Comparison of remotely sensed and modelled soil moisture data sets across Australia, *Remote Sensing of Environment*, 186, 479–500, <https://doi.org/10.1016/j.rse.2016.09.015>, 2016.
- Iwema, J., Rosolem, R., Rahman, M., Blyth, E., and Wagener, T.: Land surface model performance using cosmic-ray and point-scale soil moisture measurements for calibration, *Hydrology and Earth System Sciences*, 21, 2843–2861, <https://doi.org/10.5194/hess-21-2843-2017>, 2017.
- 660 Jackson, R. B., Canadell, J., Ehleringer, J. R., Mooney, H. A., Sala, O. E., and Schulze, E. D.: A global analysis of root distributions for terrestrial biomes, *Oecologia*, 108, 389–411, <https://doi.org/10.1007/bf00333714>, 1996.
- Jackson, T. J., Cosh, M. H., Bindlish, R., Starks, P. J., Bosch, D. D., Seyfried, M., Goodrich, D. C., Moran, M. S., and Du, J.: Validation of Advanced Microwave Scanning Radiometer Soil Moisture Products, *IEEE Transactions on Geoscience and Remote Sensing*, 48, 4256–4272, <https://doi.org/10.1109/tgrs.2010.2051035>, 2010.
- 665 Jakobi, J., Huisman, J. A., Vereecken, H., Diekkrüger, B., and Bogaen, H. R.: Cosmic Ray Neutron Sensing for Simultaneous Soil Water Content and Biomass Quantification in Drought Conditions, *Water Resources Research*, 54, 7383–7402, <https://doi.org/10.1029/2018wr022692>, 2018.
- Jost, G., Schume, H., Hager, H., Markart, G., and Kohl, B.: A hillslope scale comparison of tree species influence on soil moisture dynamics and runoff processes during intense rainfall, *Journal of Hydrology*, 420–421, 112–124, <https://doi.org/10.1016/j.jhydrol.2011.11.057>, 2012.
- 670 Kiese, R., Fersch, B., Baessler, C., Brosy, C., Butterbach-Bahl, K., Chwala, C., Dannenmann, M., Fu, J., Gasche, R., Grote, R., Jahn, C., Klatt, J., Kunstmann, H., Mauder, M., Rödiger, T., Smiatek, G., Soltani, M., Steinbrecher, R., Völsch, I., Werhahn, J., Wolf, B., Zeeman, M., and Schmid, H.: The TERENO Pre-Alpine Observatory: Integrating Meteorological, Hydrological, and Biogeochemical Measurements and Modeling, *Vadose Zone Journal*, 17, 180 060, <https://doi.org/10.2136/vzj2018.03.0060>, 2018.



- 675 Kodama, M., Nakai, K., Kawasaki, S., and Wada, M.: An application of cosmic-ray neutron measurements to the determination of the snow-water equivalent, *Journal of Hydrology*, 41, 85–92, [https://doi.org/10.1016/0022-1694\(79\)90107-0](https://doi.org/10.1016/0022-1694(79)90107-0), 1979.
- Kodama, M., Kudo, S., and Kosuge, T.: Application of atmospheric neutrons to soil moisture measurement, *Soil Science*, 140, 237–242, 1985.
- Köhli, M., Schrön, M., Zreda, M., Schmidt, U., Dietrich, P., and Zacharias, S.: Footprint characteristics revised for field-scale soil moisture
680 monitoring with cosmic-ray neutrons, *Water Resources Research*, 51, 5772–5790, <https://doi.org/10.1002/2015wr017169>, 2015.
- Köhli, M., Weimar, J., Schrön, M., Baatz, R., and Schmidt, U.: Soil Moisture and Air Humidity Dependence of the Above-Ground Cosmic-Ray Neutron Intensity, *Frontiers in Water*, 2, <https://doi.org/10.3389/frwa.2020.544847>, 2021.
- LAIV-MV - State Agency for Interior Administration Mecklenburg-Western Pomerania: Digital elevation model: ATKIS-DEM1 (© GeoBasis-DE/M-V 2011), <https://www.laiv-mv.de/Geoinformation/Geobasisdaten/Gelaendemodelle/>, 2011.
- 685 Li, D., Schrön, M., Köhli, M., Bogena, H., Weimar, J., Bello, M. A. J., Han, X., Gimeno, M. A. M., Zacharias, S., Vereecken, H., and Franssen, H.-J. H.: Can Drip Irrigation be Scheduled with Cosmic-Ray Neutron Sensing?, *Vadose Zone Journal*, 18, 190053, <https://doi.org/10.2136/vzj2019.05.0053>, 2019a.
- Li, J. and Zhang, L.: Comparison of Four Methods for Vertical Extrapolation of Soil Moisture Contents from Surface to Deep Layers in an Alpine Area, *Sustainability*, 13, 8862, <https://doi.org/10.3390/su13168862>, 2021.
- 690 Li, X., Gentine, P., Lin, C., Zhou, S., Sun, Z., Zheng, Y., Liu, J., and Zheng, C.: A simple and objective method to partition evapotranspiration into transpiration and evaporation at eddy-covariance sites, *Agricultural and Forest Meteorology*, 265, 171–182, <https://doi.org/10.1016/j.agrformet.2018.11.017>, 2019b.
- Manfreda, S., Brocca, L., Moramarco, T., Melone, F., and Sheffield, J.: A physically based approach for the estimation of root-zone soil moisture from surface measurements, *Hydrology and Earth System Sciences*, 18, 1199–1212, <https://doi.org/10.5194/hess-18-1199-2014>,
695 2014.
- Mares, V., Brall, T., Bütikofer, R., and Rühm, W.: Influence of environmental parameters on secondary cosmic ray neutrons at high-altitude research stations at Jungfrauoch, Switzerland, and Zugspitze, Germany, *Radiation Physics and Chemistry*, 168, 108557, <https://doi.org/10.1016/j.radphyschem.2019.108557>, 2020.
- Maysonave, J., Delpierre, N., François, C., Jourdan, M., Cornut, I., Bazot, S., Vincent, G., Morfin, A., and Berveiller, D.: Contribution of
700 deep soil layers to the transpiration of a temperate deciduous forest: Implications for the modelling of productivity, *Science of The Total Environment*, 838, 155981, <https://doi.org/10.1016/j.scitotenv.2022.155981>, 2022.
- McJannet, D., Hawdon, A., Baker, B., Renzullo, L., and Searle, R.: Multiscale soil moisture estimates using static and roving cosmic-ray soil moisture sensors, *Hydrology and Earth System Sciences*, 21, 6049–6067, <https://doi.org/10.5194/hess-21-6049-2017>, 2017.
- Montzka, C., Bogena, H., Zreda, M., Monerris, A., Morrison, R., Muddu, S., and Vereecken, H.: Validation of Spaceborne and Modelled
705 Surface Soil Moisture Products with Cosmic-Ray Neutron Probes, *Remote Sensing*, 9, 103, <https://doi.org/10.3390/rs9020103>, 2017.
- Neumann, R. B. and Cardon, Z. G.: The magnitude of hydraulic redistribution by plant roots: a review and synthesis of empirical and modeling studies, *New Phytologist*, 194, 337–352, <https://doi.org/10.1111/j.1469-8137.2012.04088.x>, 2012.
- Nguyen, H. H., Jeong, J., and Choi, M.: Extension of cosmic-ray neutron probe measurement depth for improving field scale root-zone soil moisture estimation by coupling with representative in-situ sensors, *Journal of Hydrology*, 571, 679–696,
710 <https://doi.org/10.1016/j.jhydrol.2019.02.018>, 2019.
- Nimmo, J. R.: The processes of preferential flow in the unsaturated zone, *Soil Science Society of America Journal*, 85, 1–27, <https://doi.org/10.1002/saj2.20143>, 2021.



- Patil, A. and Ramsankaran, R.: Improved streamflow simulations by coupling soil moisture analytical relationship in EnKF based hydrological data assimilation framework, *Advances in Water Resources*, 121, 173–188, <https://doi.org/10.1016/j.advwatres.2018.08.010>, 2018.
- 715 Paul-Limoges, E., Wolf, S., Schneider, F. D., Longo, M., Moorcroft, P., Gharun, M., and Damm, A.: Partitioning evapotranspiration with concurrent eddy covariance measurements in a mixed forest, *Agricultural and Forest Meteorology*, 280, 107786, <https://doi.org/10.1016/j.agrformet.2019.107786>, 2020.
- Peterson, A. M., Helgason, W. D., and Ireson, A. M.: Estimating field-scale root zone soil moisture using the cosmic-ray neutron probe, *Hydrology and Earth System Sciences*, 20, 1373–1385, <https://doi.org/10.5194/hess-20-1373-2016>, 2016.
- 720 Pierret, A., Maeght, J.-L., Clément, C., Montoroi, J.-P., Hartmann, C., and Gonkhamdee, S.: Understanding deep roots and their functions in ecosystems: an advocacy for more unconventional research, *Annals of Botany*, 118, 621–635, <https://doi.org/10.1093/aob/mcw130>, 2016.
- Poggio, L., de Sousa, L. M., Batjes, N. H., Heuvelink, G. B. M., Kempen, B., Ribeiro, E., and Rossiter, D.: SoilGrids 2.0: producing soil information for the globe with quantified spatial uncertainty, *SOIL*, 7, 217–240, <https://doi.org/10.5194/soil-7-217-2021>, 2021.
- R Core Team: R: A Language and Environment for Statistical Computing, R Foundation for Statistical Computing, Vienna, Austria, r version 725 3.5.1 (2018-07-02) edn., <https://www.R-project.org/>, 2018.
- R Core Team: R: A Language and Environment for Statistical Computing, R Foundation for Statistical Computing, Vienna, Austria, r version 4.3.2 (2023-10-31 ucrt) edn., <https://www.R-project.org/>, 2023.
- Rasche, D., Weimar, J., Schrön, M., Köhli, M., Morgner, M., Güntner, A., and Blume, T.: A change in perspective: downhole cosmic-ray neutron sensing for the estimation of soil moisture, *Hydrology and Earth System Sciences*, 27, 3059–3082, [https://doi.org/10.5194/hess-](https://doi.org/10.5194/hess-27-3059-2023)
730 [27-3059-2023](https://doi.org/10.5194/hess-27-3059-2023), 2023.
- Rosolem, R., Shuttleworth, W. J., Zreda, M., Franz, T. E., Zeng, X., and Kurc, S. A.: The Effect of Atmospheric Water Vapor on Neutron Count in the Cosmic-Ray Soil Moisture Observing System, *Journal of Hydrometeorology*, 14, 1659–1671, [https://doi.org/10.1175/jhm-d-](https://doi.org/10.1175/jhm-d-12-0120.1)
12-0120.1, 2013.
- Schattan, P., Baroni, G., Oswald, S. E., Schöber, J., Fey, C., Kormann, C., Huttenlau, M., and Achleitner, S.: Continuous monitoring of snowpack dynamics in alpine terrain by aboveground neutron sensing, *Water Resources Research*, 53, 3615–3634, <https://doi.org/10.1002/2016wr020234>, 2017.
- 735 Schattan, P., Köhli, M., Schrön, M., Baroni, G., and Oswald, S. E.: Sensing Area-Average Snow Water Equivalent with Cosmic-Ray Neutrons: The Influence of Fractional Snow Cover, *Water Resources Research*, 55, 10796–10812, <https://doi.org/10.1029/2019wr025647>, 2019.
- Schrön, M., Köhli, M., Scheffele, L., Iwema, J., Bogena, H. R., Lv, L., Martini, E., Baroni, G., Rosolem, R., Weimar, J., Mai, J., Cuntz, 740 M., Rebmann, C., Oswald, S. E., Dietrich, P., Schmidt, U., and Zacharias, S.: Improving calibration and validation of cosmic-ray neutron sensors in the light of spatial sensitivity, *Hydrology and Earth System Sciences*, 21, 5009–5030, [https://doi.org/10.5194/hess-21-5009-](https://doi.org/10.5194/hess-21-5009-2017)
2017, 2017.
- Schrön, M., Rosolem, R., Köhli, M., Piussi, L., Schröter, I., Iwema, J., Kögler, S., Oswald, S. E., Wollschläger, U., Samaniego, L., Dietrich, P., and Zacharias, S.: Cosmic-ray Neutron Rover Surveys of Field Soil Moisture and the Influence of Roads, *Water Resources Research*, 745 54, 6441–6459, <https://doi.org/10.1029/2017wr021719>, 2018a.
- Schrön, M., Zacharias, S., Womack, G., Köhli, M., Desilets, D., Oswald, S. E., Bumberger, J., Mollenhauer, H., Kögler, S., Remmler, P., Kasner, M., Denk, A., and Dietrich, P.: Intercomparison of cosmic-ray neutron sensors and water balance monitoring in an urban environment, *Geoscientific Instrumentation, Methods and Data Systems*, 7, 83–99, <https://doi.org/10.5194/gi-7-83-2018>, 2018b.
- Schrön, M., Oswald, S. E., Zacharias, S., Kasner, M., Dietrich, P., and Attinger, S.: Neutrons on Rails: Transregional Monitoring of Soil 750 Moisture and Snow Water Equivalent, *Geophysical Research Letters*, 48, <https://doi.org/10.1029/2021gl093924>, 2021.



- Schume, H., Jost, G., and Katzensteiner, K.: Spatio-temporal analysis of the soil water content in a mixed Norway spruce (*Picea abies* (L.) Karst.)–European beech (*Fagus sylvatica* L.) stand, *Geoderma*, 112, 273–287, [https://doi.org/10.1016/s0016-7061\(02\)00311-7](https://doi.org/10.1016/s0016-7061(02)00311-7), 2003.
- Seneviratne, S. I., Corti, T., Davin, E. L., Hirschi, M., Jaeger, E. B., Lehner, I., Orlowsky, B., and Teuling, A. J.: Investigating soil moisture–climate interactions in a changing climate: A review, *Earth-Science Reviews*, 99, 125–161, <https://doi.org/10.1016/j.earscirev.2010.02.004>, 2010.
- 755 Sponagel, H., Grotenthaler, W., Hartmann, K.-J., Hartwich, R., Janetzko, P., Joisten, H., Kühn, D., Sabel, K.-J., and Traidl, R.: Bodenkundliche Kartieranleitung KA5, BGR - German Federal Institute for Geosciences and Natural Resources, Hannover, Germany, 5 edn., 2005.
- Stevanato, L., Baroni, G., Cohen, Y., Lino, F. C., Gatto, S., Lunardon, M., Marinello, F., Moretto, S., and Morselli, L.: A Novel Cosmic-Ray Neutron Sensor for Soil Moisture Estimation over Large Areas, *Agriculture*, 9, 202, <https://doi.org/10.3390/agriculture9090202>, 2019.
- 760 Tian, Z., Li, Z., Liu, G., Li, B., and Ren, T.: Soil water content determination with cosmic-ray neutron sensor: Correcting aboveground hydrogen effects with thermal/fast neutron ratio, *Journal of Hydrology*, 540, 923–933, <https://doi.org/10.1016/j.jhydrol.2016.07.004>, 2016.
- Vather, T., Everson, C., and Franz, T. E.: Calibration and Validation of the Cosmic Ray Neutron Rover for Soil Water Mapping within Two South African Land Classes, *Hydrology*, 6, 65, <https://doi.org/10.3390/hydrology6030065>, 2019.
- 765 Vather, T., Everson, C. S., and Franz, T. E.: The Applicability of the Cosmic Ray Neutron Sensor to Simultaneously Monitor Soil Water Content and Biomass in an *Acacia mearnsii* Forest, *Hydrology*, 7, 48, <https://doi.org/10.3390/hydrology7030048>, 2020.
- Vereecken, H., Huisman, J. A., Bogaen, H., Vanderborght, J., Vrugt, J. A., and Hopmans, J. W.: On the value of soil moisture measurements in vadose zone hydrology: A review, *Water Resources Research*, 44, <https://doi.org/10.1029/2008wr006829>, 2008.
- Vereecken, H., Huisman, J., Pachepsky, Y., Montzka, C., van der Kruk, J., Bogaen, H., Weihermüller, L., Herbst, M., Martinez, G., and Vanderborght, J.: On the spatio-temporal dynamics of soil moisture at the field scale, *Journal of Hydrology*, 516, 76–96, <https://doi.org/10.1016/j.jhydrol.2013.11.061>, 2014.
- 770 Wagner, W., Lemoine, G., and Rott, H.: A Method for Estimating Soil Moisture from ERS Scatterometer and Soil Data, *Remote Sensing of Environment*, 70, 191–207, [https://doi.org/10.1016/s0034-4257\(99\)00036-x](https://doi.org/10.1016/s0034-4257(99)00036-x), 1999.
- Wang, C., Fu, B., Zhang, L., and Xu, Z.: Soil moisture–plant interactions: an ecohydrological review, *Journal of Soils and Sediments*, 19, 1–9, <https://doi.org/10.1007/s11368-018-2167-0>, 2018.
- 775 Weimar, J., Köhli, M., Budach, C., and Schmidt, U.: Large-Scale Boron-Lined Neutron Detection Systems as a ^3He Alternative for Cosmic Ray Neutron Sensing, *Frontiers in Water*, 2, 16, <https://doi.org/10.3389/frwa.2020.00016>, 2020.
- Zacharias, S., Bogaen, H., Samaniego, L., Mauder, M., Fuß, R., Pütz, T., Frenzel, M., Schwank, M., Baessler, C., Butterbach-Bahl, K., Bens, O., Borg, E., Brauer, A., Dietrich, P., Hajnsek, I., Helle, G., Kiese, R., Kunstmann, H., Klotz, S., Munch, J. C., Papen, H., Priesack, E., Schmid, H. P., Steinbrecher, R., Rosenbaum, U., Teutsch, G., and Vereecken, H.: A Network of Terrestrial Environmental Observatories in Germany, *Vadose Zone Journal*, 10, 955–973, <https://doi.org/10.2136/vzj2010.0139>, 2011.
- 780 Zambrano-Bigiarini, M.: hydroGOF: Goodness-of-fit functions for comparison of simulated and observed hydrological time series, <https://doi.org/https://zenodo.org/records/840087>, r package version 0.3-10, 2017.
- Zambrano-Bigiarini, M.: hydroGOF: Goodness-of-fit functions for comparison of simulated and observed hydrological time series, <https://doi.org/https://zenodo.org/records/3707013>, r package version 0.4-0, 2020.
- 785 Zhang, N., Quiring, S., Ochsner, T., and Ford, T.: Comparison of Three Methods for Vertical Extrapolation of Soil Moisture in Oklahoma, *Vadose Zone Journal*, 16, [vzj2017.04.0085](https://doi.org/10.2136/vzj2017.04.0085), <https://doi.org/10.2136/vzj2017.04.0085>, 2017.



- Zhu, X., Shao, M., Jia, X., Huang, L., Zhu, J., and Zhang, Y.: Application of temporal stability analysis in depth-scaling estimated soil water content by cosmic-ray neutron probe on the northern Tibetan Plateau, *Journal of Hydrology*, 546, 299–308, 790 <https://doi.org/10.1016/j.jhydrol.2017.01.019>, 2017.
- Zhuang, R., Zeng, Y., Manfreda, S., and Su, Z.: Quantifying Long-Term Land Surface and Root Zone Soil Moisture over Tibetan Plateau, *Remote Sensing*, 12, 509, <https://doi.org/10.3390/rs12030509>, 2020.
- Zreda, M., Desilets, D., Ferré, T. P. A., and Scott, R. L.: Measuring soil moisture content non-invasively at intermediate spatial scale using cosmic-ray neutrons, *Geophysical Research Letters*, 35, <https://doi.org/10.1029/2008gl035655>, 2008.
- 795 Zreda, M., Shuttleworth, W. J., Zeng, X., Zweck, C., Desilets, D., Franz, T., and Rosolem, R.: COSMOS: the COsmic-ray Soil Moisture Observing System, *Hydrology and Earth System Sciences*, 16, 4079–4099, <https://doi.org/10.5194/hess-16-4079-2012>, 2012.